– Supporting Information –

Double Metal Cyanide (DMC) Catalysis: Detailed *in situ* NMR Kinetics Studies on the Copolymerization of Propylene Oxide with Substituted Epoxides

Erik Kersten[†], Maximilian Kaiser[†], Jan Blankenburg[†§], Kamil Maciol[†], Manfred Wagner[‡], Sirus Zarbakhsh[¥], Holger Frey[†,*]

[†]Department of Chemistry, Johannes Gutenberg-University, Duesbergweg 10-14, 55128 Mainz, Germany

§ Graduate School Materials Science in Mainz, Staudinger Weg 9, 55128 Mainz, Germany

[‡]Max-Planck-Institute for Polymer Research, Ackermannweg 10, 55128 Mainz

[¥]BASF SE, Carl-Bosch-Straße 38, 67056 Ludwigshafen am Rhein, Germany

*E-Mail: hfrey@uni-mainz.de

J.B., E.K. and M.K. contributed equally to this work.

Experimentals

Reagents. All solvents and reagents were generally purchased from Acros Organics, TCI, Sigma-Aldrich, or Fluka and used as received, if not otherwise mentioned. The polymerizations were carried out using a heterogeneous cobalt–zinc double metal cyanide (DMC) catalyst of the zinc hexacyanocobaltate type, provided by BASF SE and commonly applied in industrial polyether polyol synthesis. The catalyst is a crystalline, non-air-sensitive solid with a platelet-like morphology and micrometer-sized particles. Deuterated solvents and deuterated propylene oxide were received from Deutero GmbH. Propylene oxide (PO) and all comonomers were stirred over calcium hydride and distilled into a Schlenk flask with molecular sieves 3 Å before use.

Synthesis of ethoxy ethyl glycidyl ether (EEGE). EEGE was prepared according to the synthesis protocol by Fitton and others.[1]

Synthesis of ethoxy butoxy vinyl glycidyl ether (EBVGE). EBVGE was synthesized according to a synthesis procedure described by Maciol and others.[2] To a 100 mL flask equipped with stir bar, glycidol (1 eq.) and 1,4-butanedio divinyl ether (3 eq.) were added and the mixture was cooled to 0 °C. Subsequently *p*-toluenesulfonic acid monohydrate (0.01 eq.) were added and the mixture was allowed to reach room temperature. After stirring for four hours, the mixture was washed with aqueous $NaHCO_3$ solution (3 x 20 mL) and the organic phase was separated and dried over anhydrous K_2CO_3. Following distillation under reduced pressure, the product EBVGE was obtained as a colorless liquid in a yield of 69 %.

Synthesis of glycidyl benzoate (GBz). GBz was synthesized in an adaption to an protocol of Leuschner and others.[3] For the synthesis of potassium benzoate 18.4 g (0.15 mol; 1 eq) benzoic acid and 8.3 g (0.15 mol; 1 eq) KOH were dissolved in 150 mL THF and the mixture was stirred

for 2 hours at 30 °C. The solvent was removed under reduced pressure. The dried potassium benzoate was dissolved in 80 mL acetonitrile and 2.42 g (7.5 mmol; catalytic) tetra butyl-ammonium bromide (TBAB) and 35 mL (0.45 mol; 3 eq) epichlorohydrin were added. The suspension was stirred and heated for 3 hours at 100 °C. After filtration and washing of the solid with acetonitrile, the solvent was evaporated under reduced pressure and the residue diluted with 70 mL dichloromethane. The organic phase was washed twice with 20 mL saturated $NaHCO_3$ solution and brine. After drying with $MgSO_4$, the solid was filtered off and washed with dichloromethane. The solvent was evaporated under reduced pressure to obtain the crude product. A distillation at 110 °C under reduced pressure was conducted to isolate the pure product in 41% yield.

Size exclusion chromatography (SEC) was performed in *N,N*-dimethylformamide (DMF) with 1 g/L lithium bromide as an eluent and Polymer Standards Service (PSS) HEMA columns (300/100/40 Å porosity) at 50 °C, using a RI detector. Molecular weights were determined by a calibration with poly(ethylene oxide) standards provided by PSS.

Matrix assisted laser desorption ionization-time of flight mass spectrometry (MALDI-ToF-MS) was performed on a Bruker Rapiflex with trans-2-[3-(4-tert-Butylphenyl)-2-methyl-2-propenylidene]malononitrile (DCTB) as a matrix.

^{1}H NMR kinetic experiments. In the following, an exemplary experiment protocol for the copolymerization of PO and BO is described. All other copolymerization experiments were performed analogously. For the copolymerization experiment of PO and EEGE, the addition of a solvent was omitted. The precise ratio of PO to comonomer was individually adjusted for each

copolymerization experiment to account for the expected monomer consumption behavior and composition drift during copolymerization.

To ensure a safe handling of PO under elevated temperature in the ^{1}H NMR kinetic measurements, a special high-pressure NMR tube equipped with a valve was used (Norell S-5-500-HW-HPV-7). Drying of the initiator 1-tridecanol was performed by dissolving in benzene and applying reduced pressure over night. The preparation of the NMR tube was performed in a glovebox. In a first step a stock solution of DMC, 1-tridecanol, BO and PO in benzene-d_6 was prepared to handle the small quantities of DMC catalyst needed. For this purpose, 0.6 mg (300 ppm) of the DMC catalyst, 194 mg (0.97 mmol, 1 eq) 1-tridecanol, 1.6 mL (23 mmol, 24 eq) PO, 0.5 mL (5.7 mmol, 6 eq) BO and (0.97 g, 33 wt.%) benzene-d_6 were added to a screw cap vial, sealed and stirred for 5 min. 0.1 mL of the mixture was transferred via syringe into the sealable high-pressure NMR tube under argon atmosphere. Subsequently, the NMR tube was sealed and frozen in liquid nitrogen. Before the kinetic experiment was started, the prepared NMR tube was allowed to reach room temperature and sonicated for homogenization. The *in situ* ^{1}H NMR spectroscopy was performed at 80 °C on a Bruker Avance III BR 500/51 (500 MHz), recording a spectrum with one scan every 30 s. *^{1}H ^{2}H NMR kinetic experiment.* The kinetic NMR tube was prepared according to the procedure above. In an alternating sequence a ^{1}H spectrum at 500 MHz and a ^{2}H spectrum at 76.8 MHz were recorded.

The total duration of each kinetic experiment varied, as the measurements were continued until complete conversion of either one or both monomers had been achieved. For clarity, 76 representative ^{1}H NMR spectra acquired throughout the course of the experiment are displayed in the stacked ^{1}H NMR kinetic plots. Only monomer conversion data collected after complete temperature equilibration at 80 °C, stabilization of the NMR signals, and after the respective

individual induction period were used for the determination of the reactivity ratios. Thus, the kinetic analysis was based on the actual monomer concentration in the NMR detection volume under the reaction conditions, thereby accounting for any redistribution of PO between the liquid phase and the headspace upon heating.

Catalyst structure and proposed mechanisms

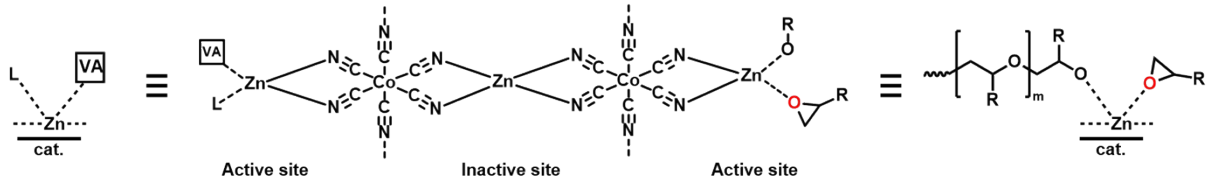

L = Coligand
VA = Vacancy site
O-R = Initiator or polymer chain hydroxy end group

Scheme S1. Proposed catalyst structure with peripheral Zn^{2+} active sites.[4]

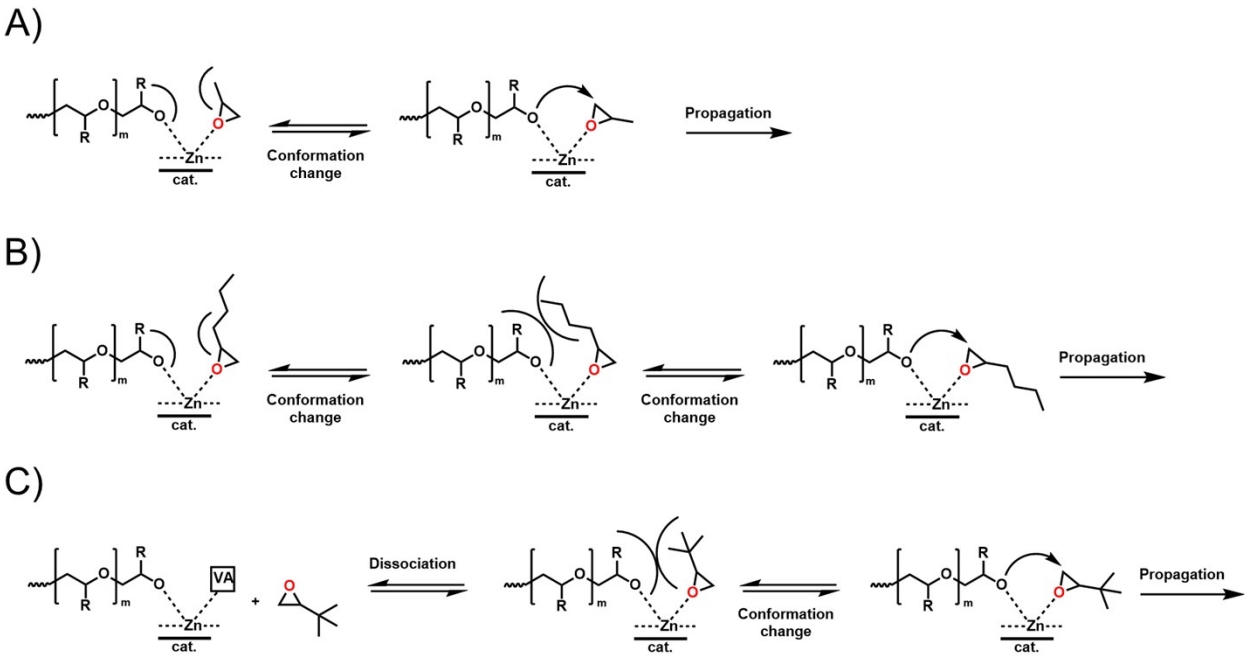

Scheme S2. Proposed influence of bulky side chains of alkylene oxides and aryl epoxides (AO) during coordination at catalyst site and propagation step.

MALDI-ToF mass spectroscopy

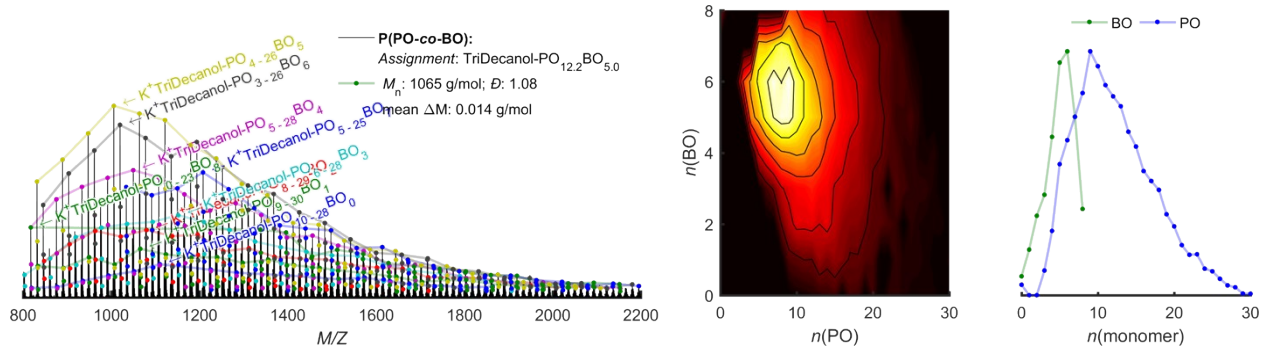

Figure S1. Left: MALDI-mass spectrum with assigned peaks of P(PO-*co*-BO) copolymer, center: 2D-composition, right: representation of the monomer distribution in 2D.

Supplementary plots and data of *in situ* copolymerization kinetics of PO with alkylene oxides and aryl epoxides (AO)

Table S1. Overview of determined molar ratio PO to comonomer in *in situ* kinetic experiments with theoretical molecular weights and molecular weights determined via SEC of the respective copolymer resulting from the copolymerization experiment.

Comonome Xr	Copolymer	$n_{PO} : m_{Co}$ [a)]	$M_n^{Theo.}$ / g mol^{-1}	M_n^{SEC} / g mol^{-1}	$Đ$
BO	P(PO_n-*co*-BO_m)	18:6	1680	1500	1.13
HexO	P(PO_n-*co*-$HexO_m$)	20:5	1860	1610	1.18
SO	P(PO_n-*co*-SO_m)	16:4	1610	1260	1.18
MEB	P(PO_n-*co*-MEB_m)	21:5	1850	1590	1.13
DMEB[b)]	P(PO_n-*co*-$DMEB_m$)	26:6	2300	n.d.	n.d
AGE	P(PO_n-*co*-AGE_m)	15:5	1640	1720	1.61
BGE	P(PO_n-*co*-BGE_m)	13:4	1610	1220	1.33
FGE	P(PO_n-*co*-FGE_m)	18:5	2020	1620	2.17
PGE	P(PO_n-*co*-PGE_m)	20:4	1960	1750	1.99
MPGE	P(PO_n-*co*-$MPGE_m$)	20:4	2020	1590	1.56
EBVGE	P(PO_n-*co*-$EBVGE_m$)	32:6	3360	1490	1.18
EEGE^{DMC,BULK}	P(PO_n-*co*-$EEGE_m$)	14:5	1740	1210	1.55
GMA[c)]	P(PO_n-*co*-GMA_m)	20:6	2220	n.d.	n.d.
GBz	P(PO_n-*co*-GBz_m)	16:4	1840	1350	1.22

[a)]molar ratio of PO to comonomer, determined from the first recorded ^{1}H NMR spectrum of the respective *in situ* kinetic experiment and internally referenced to the proton signal of the 1-tridecanol initiator.

[b)]no copolymer formation during *in situ* kinetic experiment.

[c)]could not be determined due to the insolubility of the crosslinked copolymer.

Table S2. Reactivity ratios of copolymerization of PO with alkylene oxides and aryl epoxides determined via Jaacks-fit and the fraction of apparent rate constants.

	Jaacks		k_1/k_2	k_2/k_1
Comonomer X	r_{PO}	r_X	r_{PO}	r_X
PO-d_6	1.0	1.0	1.0	0.99
EO	2.2	0.46	2.0	0.49
BO	5.6	0.18	5.8	0.17
HexO	15	0.066	15	0.069
SO	25	0.040	27	0.037
MEB	27	0.037	26	0.039

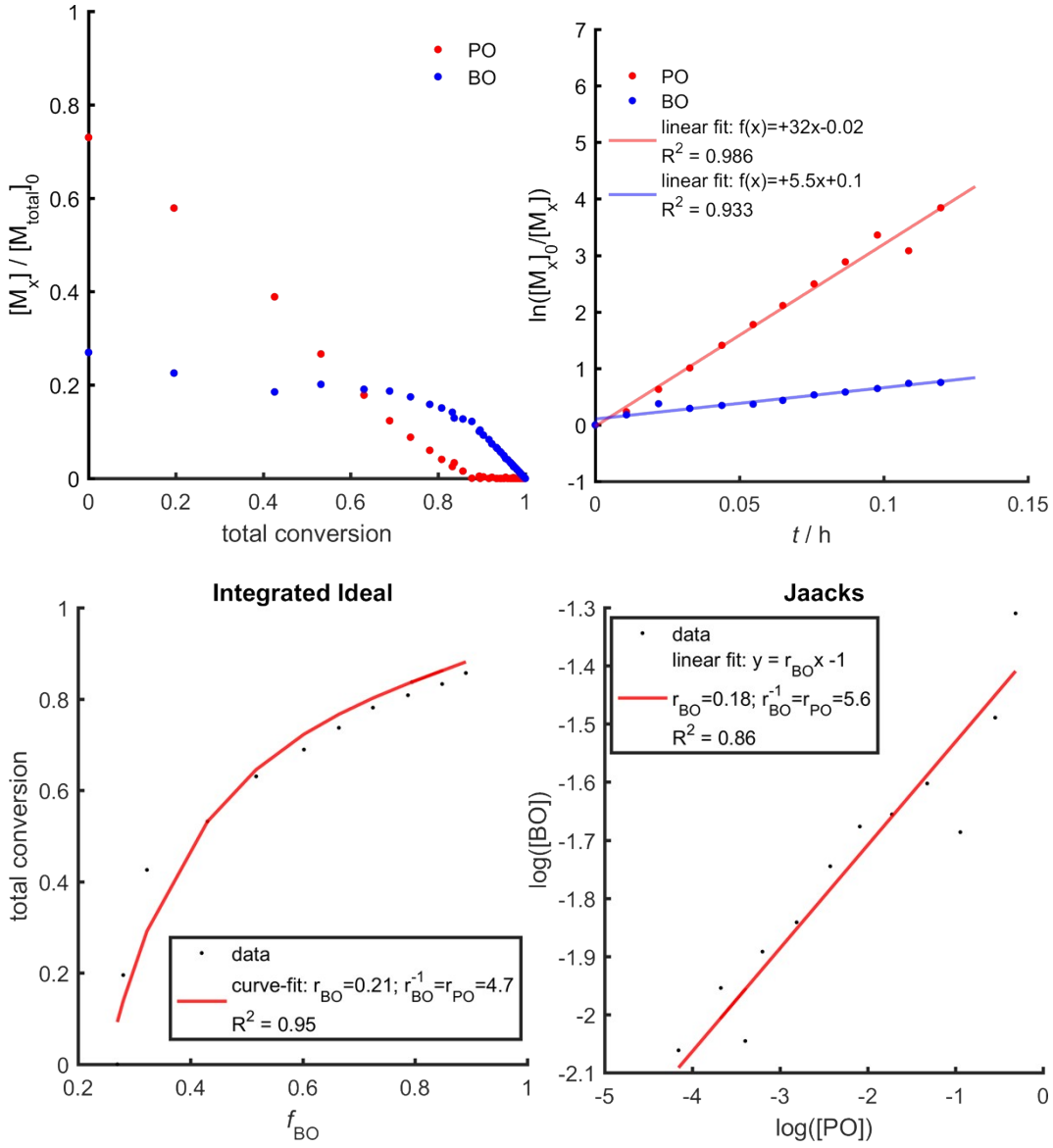

Figure S2. ^{1}H NMR PO-BO copolymerization experiment: Data with fits to obtain reactivity ratios. Only monomer conversion data in the time interval after the induction period until complete conversion of PO were fitted.

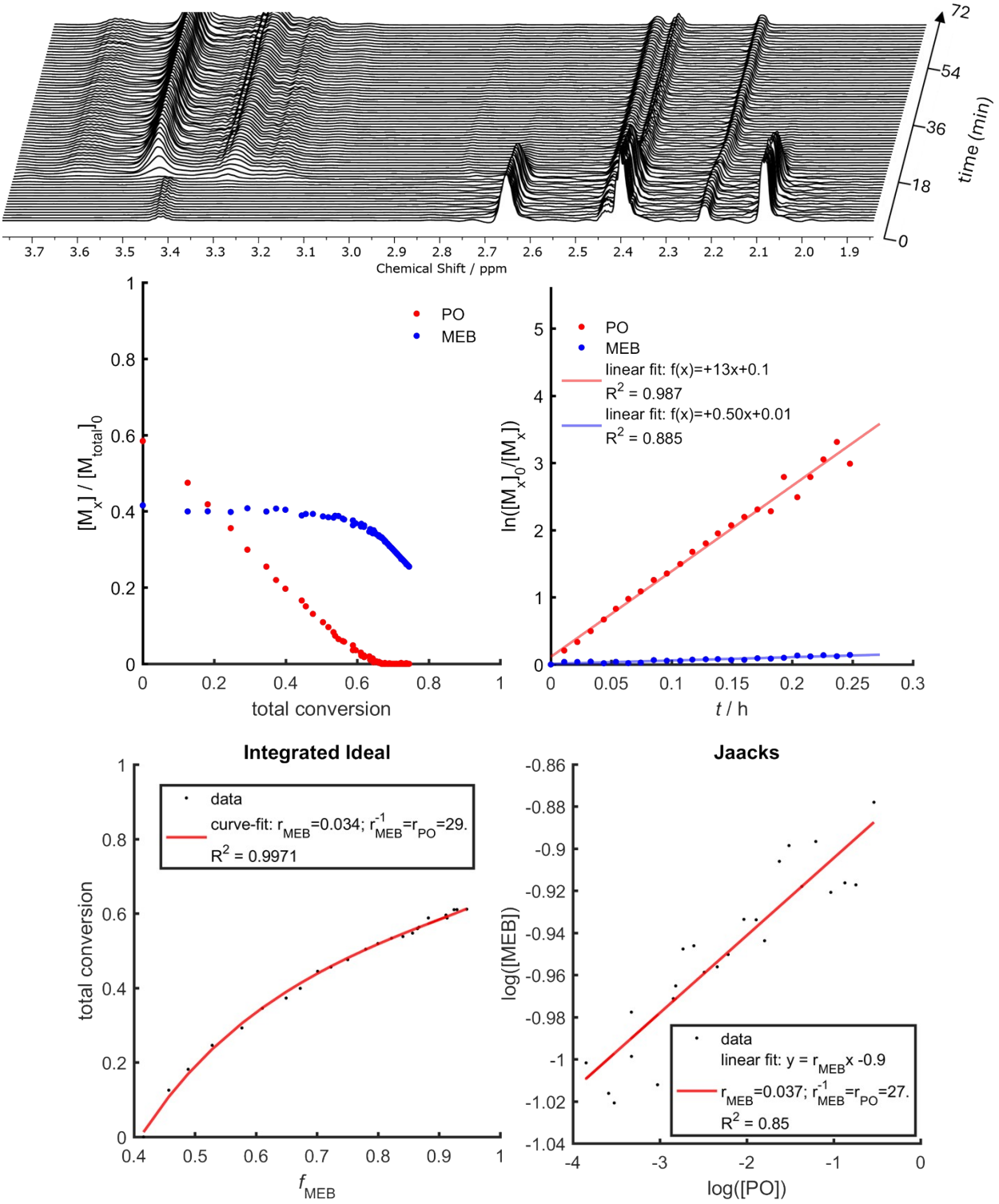

Figure S3. ^{1}H NMR PO-MEB copolymerization experiment: Data with fits to obtain reactivity ratios. Only monomer conversion data in the time interval after the induction period until complete conversion of PO were fitted.

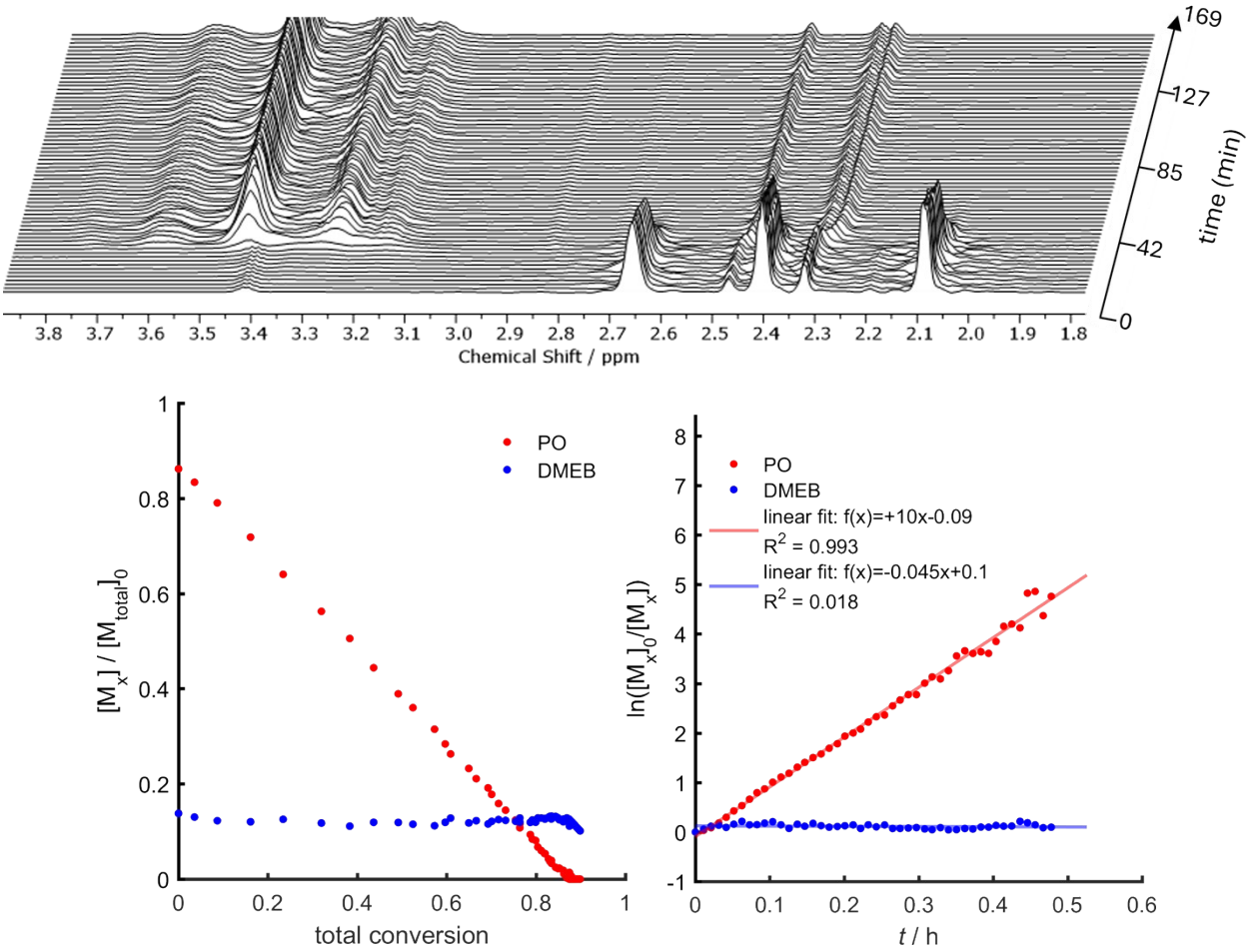

Figure S4. ^{1}H NMR PO-DMEB copolymerization experiment. Only monomer conversion data in the time interval after the induction period until complete conversion of PO were fitted.

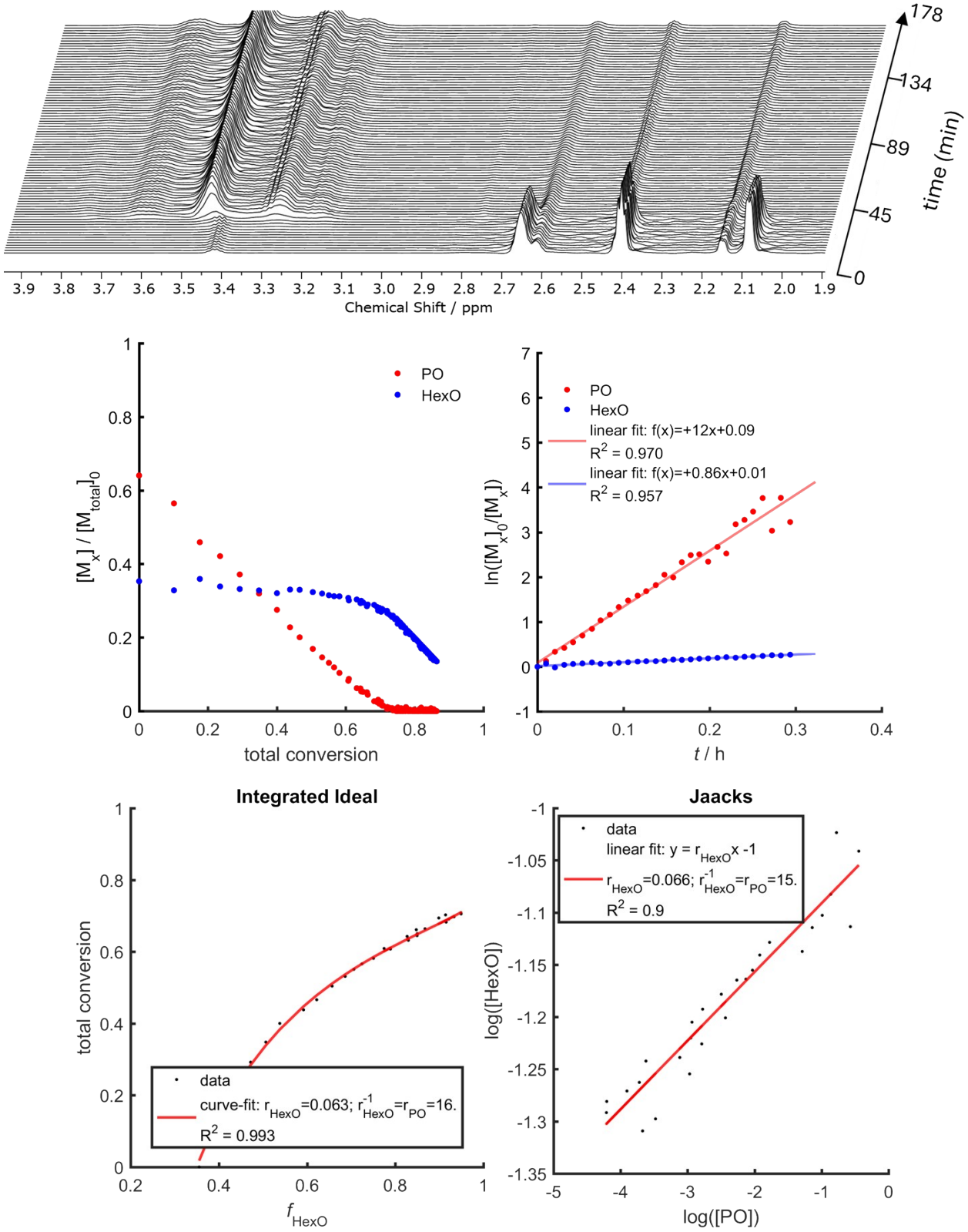

Figure S5. ^{1}H NMR PO-HexO copolymerization experiment: Data with fits to obtain reactivity ratios. Only monomer conversion data in the time interval after the induction period until complete conversion of PO were fitted.

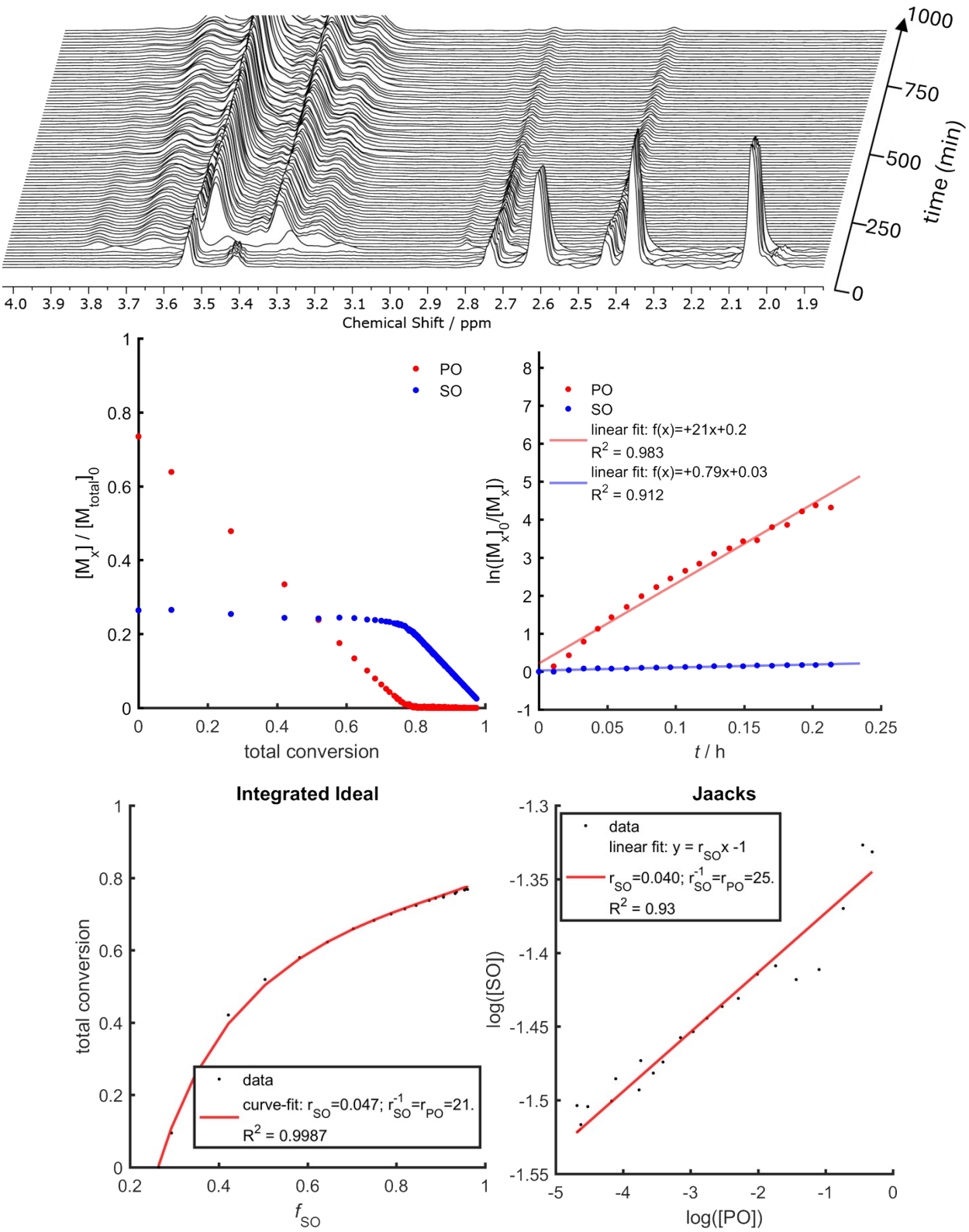

Figure S6. ^{1}H NMR PO-SO copolymerization experiment: Data with fits to obtain reactivity ratios. Only monomer conversion data in the time interval after the induction period until complete conversion of PO were fitted.

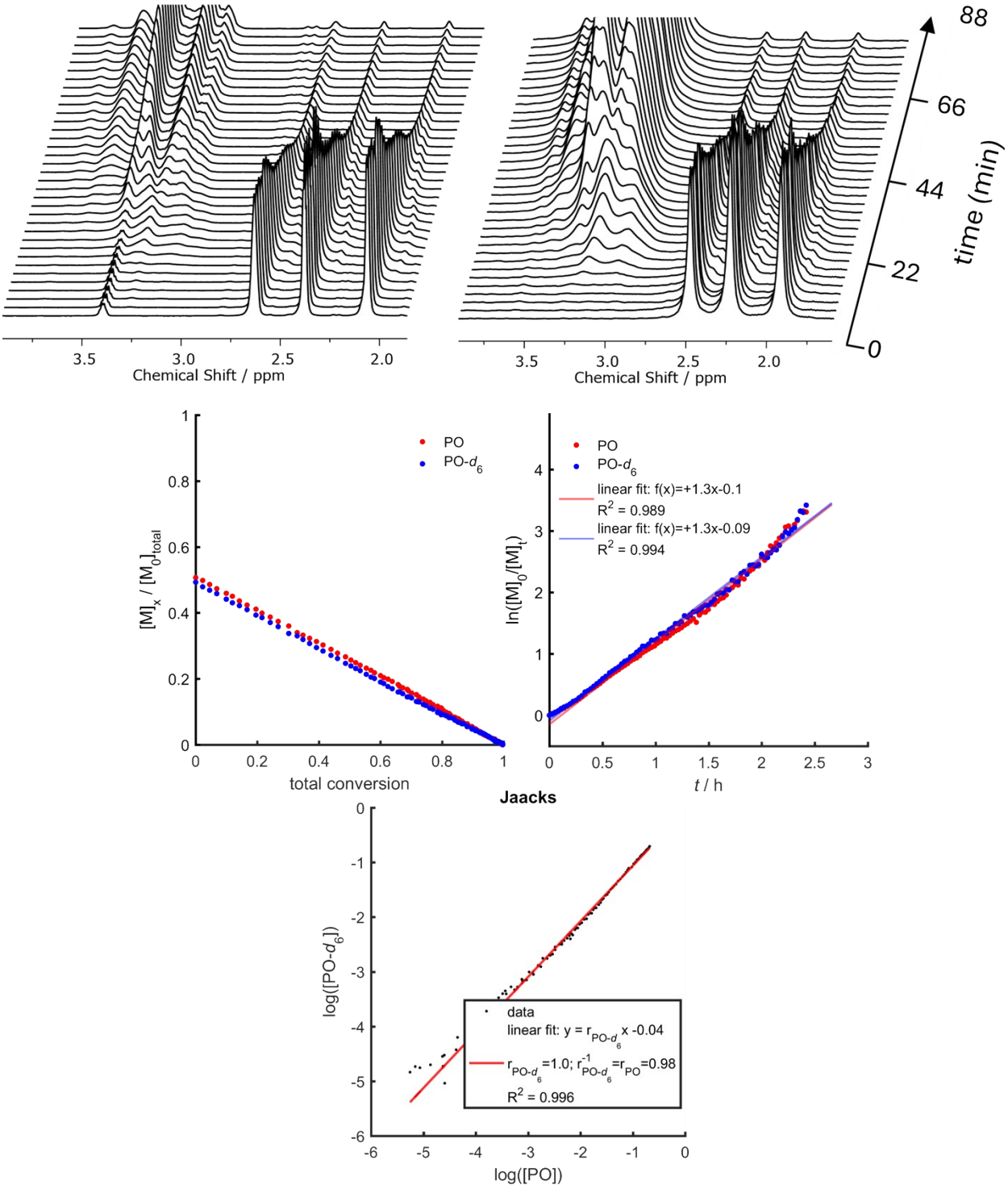

Figure S7. ^{1}H (left) and ^{2}H (right) NMR spectra of the copolymerization of PO with PO-d_6: Data with fits to obtain reactivity ratios. Only monomer conversion data in the time interval after the induction period until complete conversion of PO were fitted.

Supplementary plots and data of *in situ* copolymerization kinetics of PO with glycidyl ethers (GE) and esters (GEs)

Table S3. Reactivity ratios of copolymerization of PO with glycidyl ethers and glycidyl esters determined via Jaacks-fit and the fraction of apparent rate constants.

	Jaacks		k_1/k_2	k_2/k_1
Comonomer X	r_{PO}	r_X	r_{PO}	r_X
AGE	8.5	0.12	8.4	0.12
BGE	12	0.083	12	0.080
FGE	13	0.076	15	0.066
PGE	14	0.070	13	0.079
EBVGE	14	0.071	14	0.073
MPGE	17	0.060	16	0.064
EEGE (bulk)	20	0.049	24	0.042
GMA	21	0.048	19	0.051
Gbz	32	0.031	33	0.031

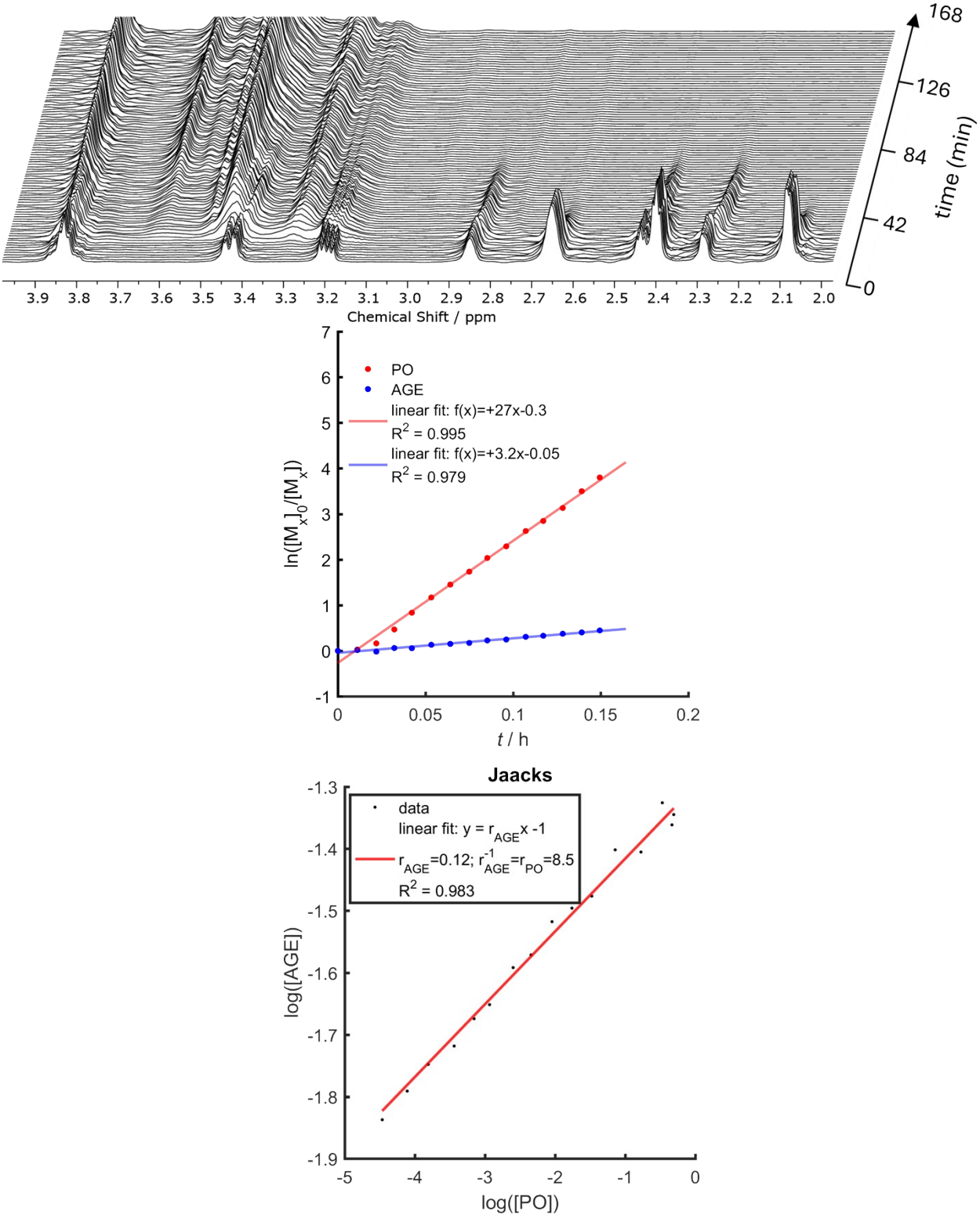

Figure S8. ^{1}H NMR PO-AGE copolymerization experiment: Data with fits to obtain reactivity ratios. Only monomer conversion data in the time interval after the induction period until complete conversion of PO were fitted.

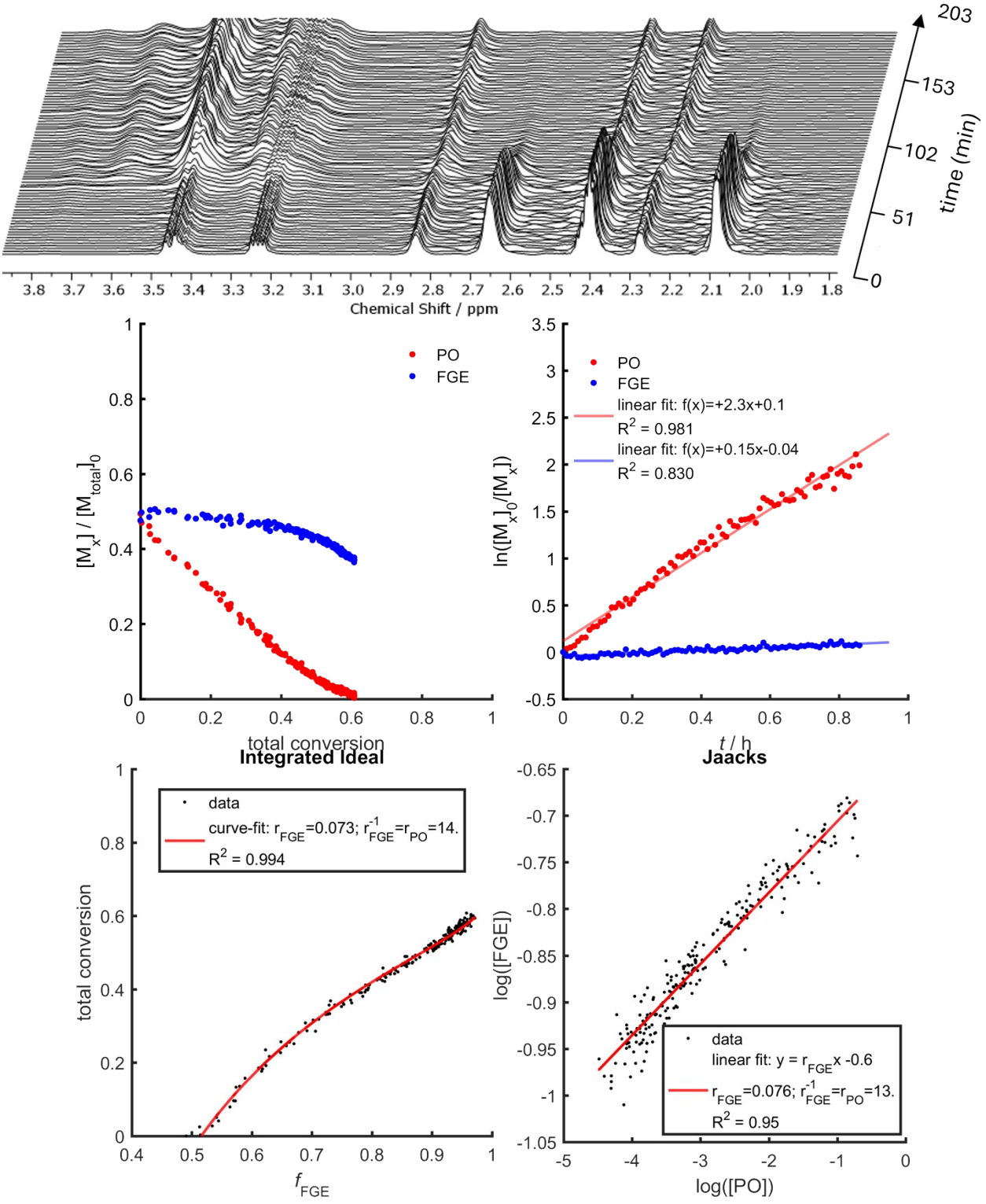

Figure S9. ^{1}H NMR PO-FGE copolymerization experiment: Data with fits to obtain reactivity ratios. Only monomer conversion data in the time interval after the induction period until complete conversion of PO were fitted.

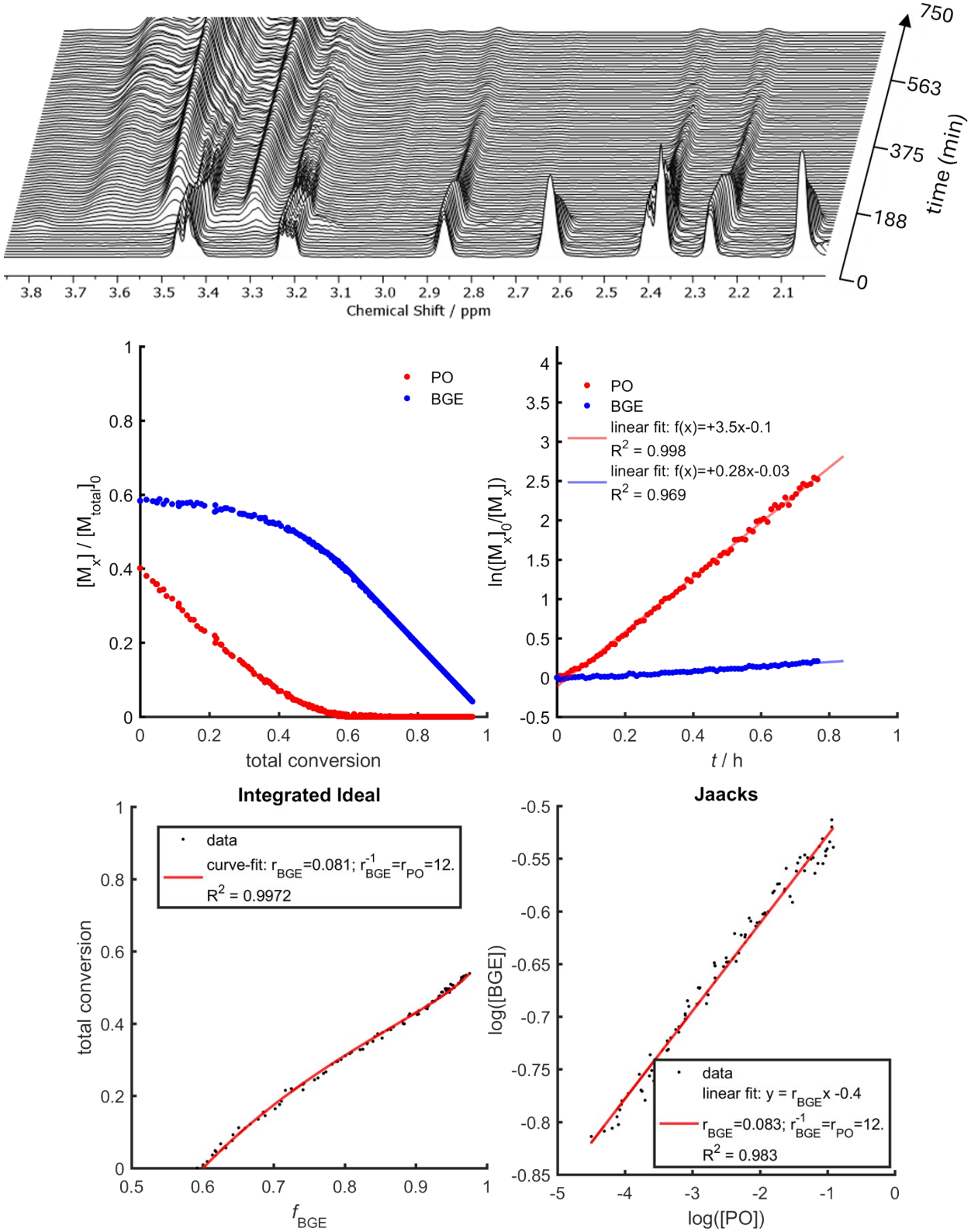

Figure S10. [1]H NMR PO-BGE copolymerization experiment: Data with fits to obtain reactivity ratios. Only monomer conversion data in the time interval after the induction period until complete conversion of PO were fitted.

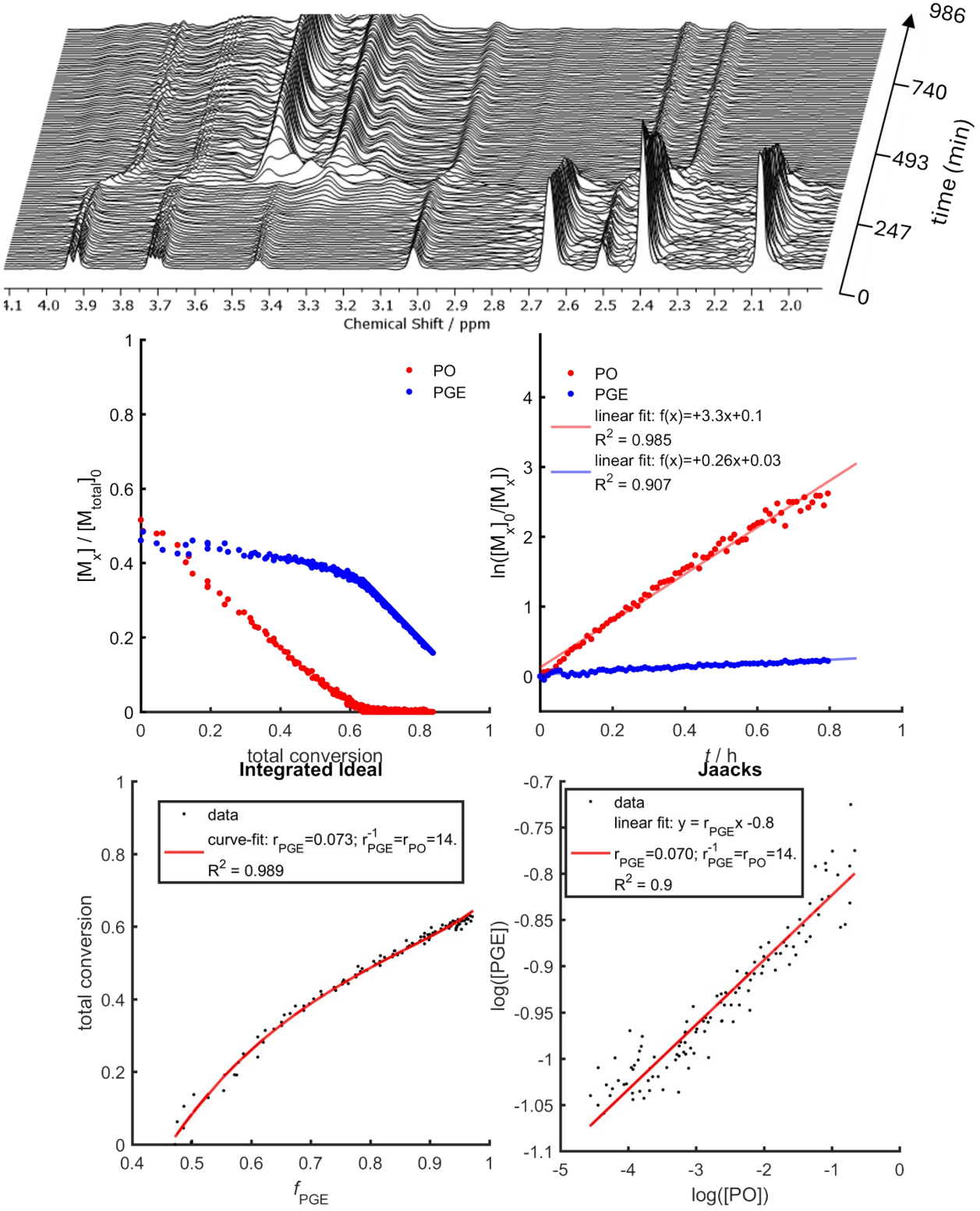

Figure S11. ^{1}H NMR PO-PGE copolymerization experiment: Data with fits to obtain reactivity ratios. Only monomer conversion data in the time interval after the induction period until complete conversion of PO were fitted.

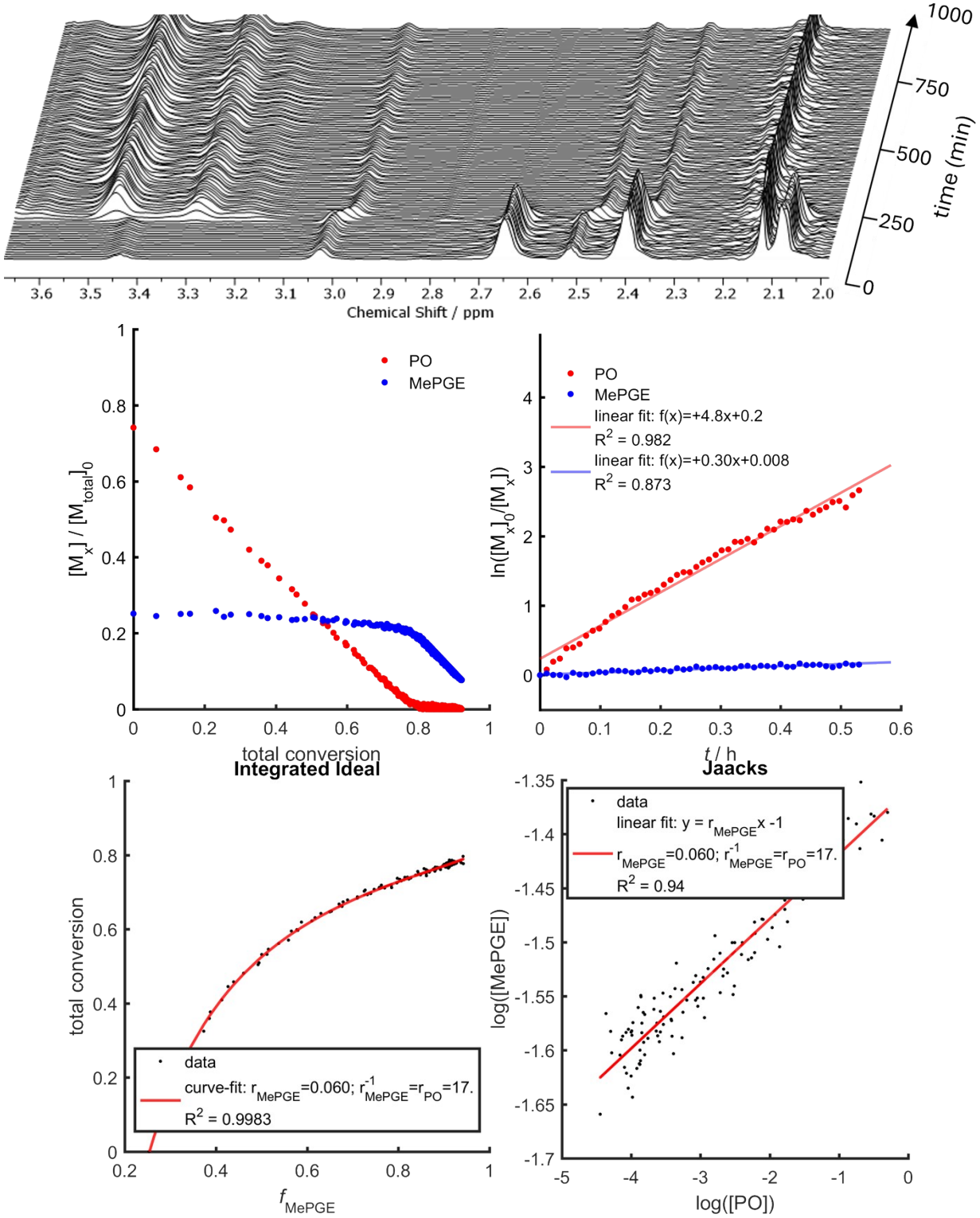

Figure S12. ^{1}H NMR PO-MPGE copolymerization experiment: Data with fits to obtain reactivity ratios. Only monomer conversion data in the time interval after the induction period until complete conversion of PO were fitted.

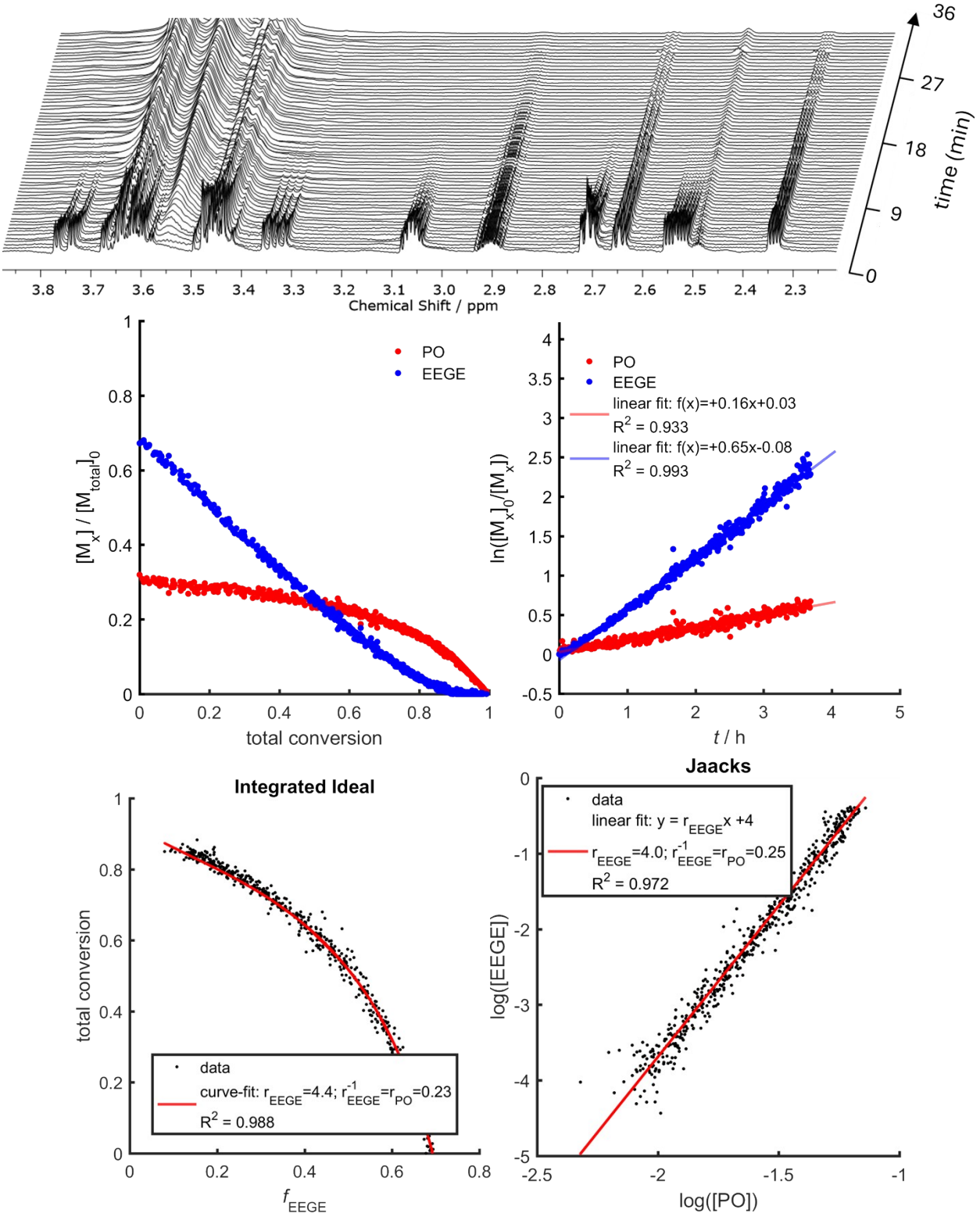

Figure S13. ^{1}H NMR PO-EEGE (AROP) copolymerization experiment: Data with fits to obtain reactivity ratios. Only monomer conversion data in the time interval after the induction period until complete conversion of PO were fitted.

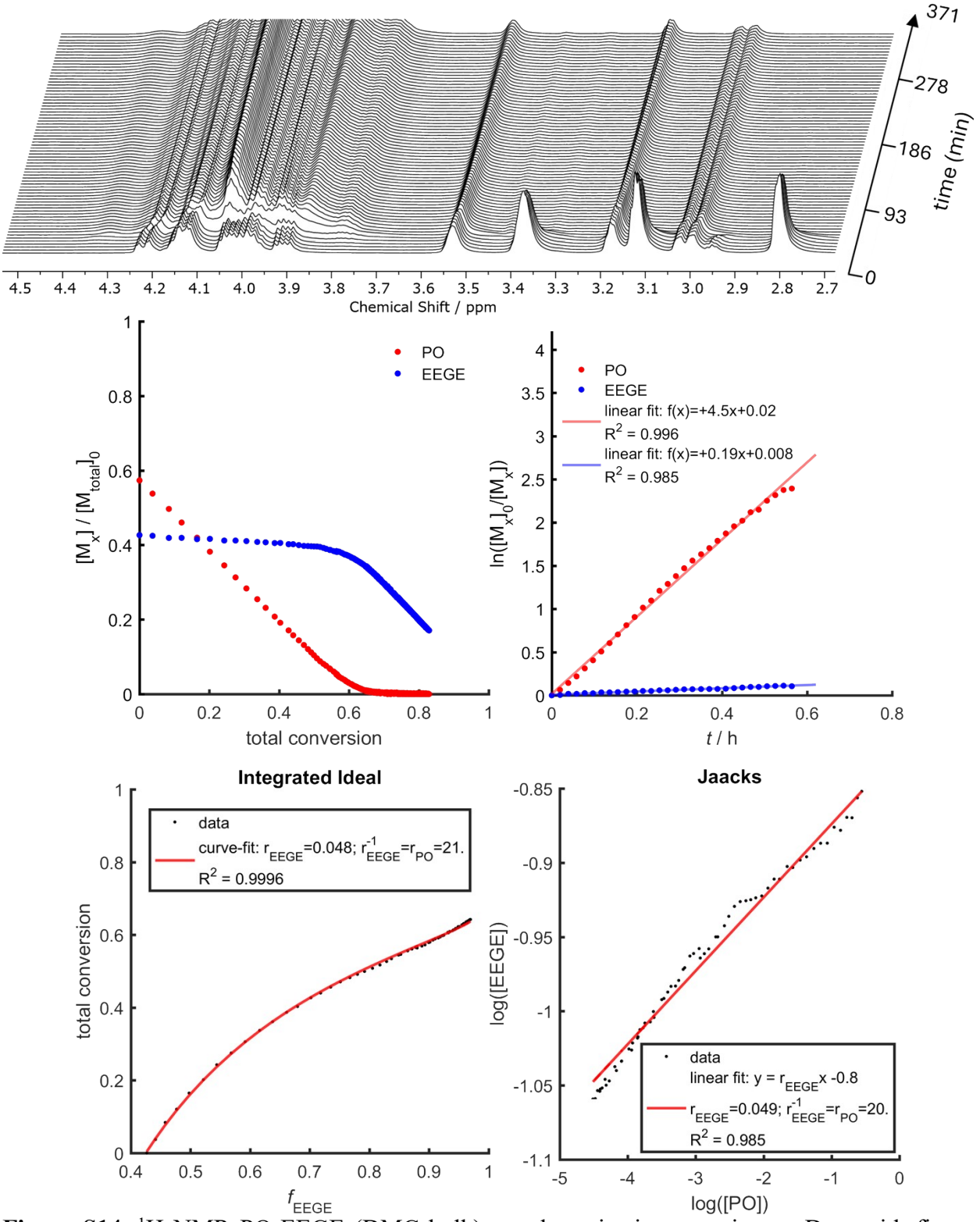

Figure S14. ^{1}H NMR PO-EEGE (DMC bulk) copolymerization experiment: Data with fits to obtain reactivity ratios. Only monomer conversion data in the time interval after the induction period until complete conversion of PO were fitted.

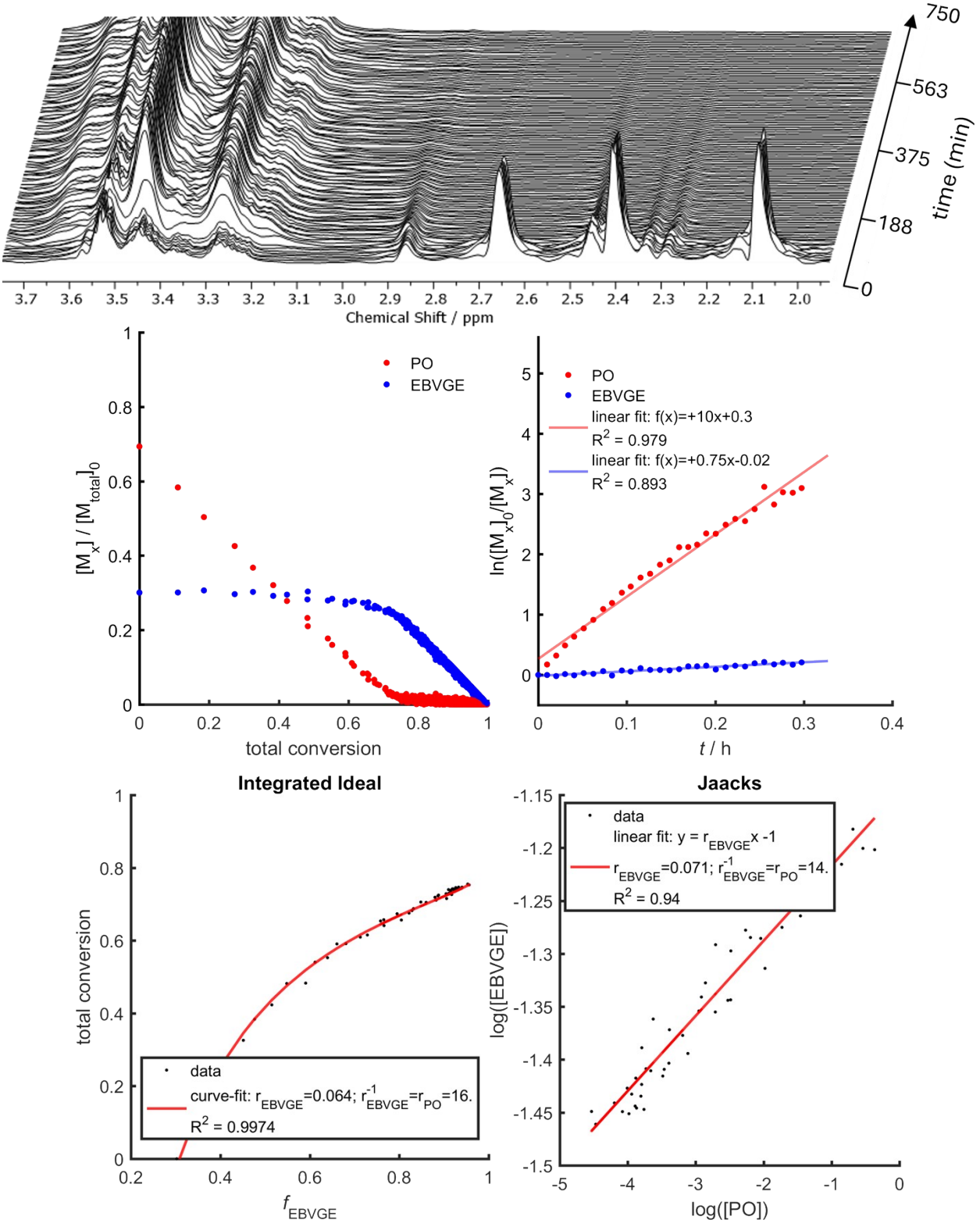

Figure S15. ^{1}H NMR PO-EBVGE copolymerization experiment: Data with fits to obtain reactivity ratios. Only monomer conversion data in the time interval after the induction period until complete conversion of PO were fitted.

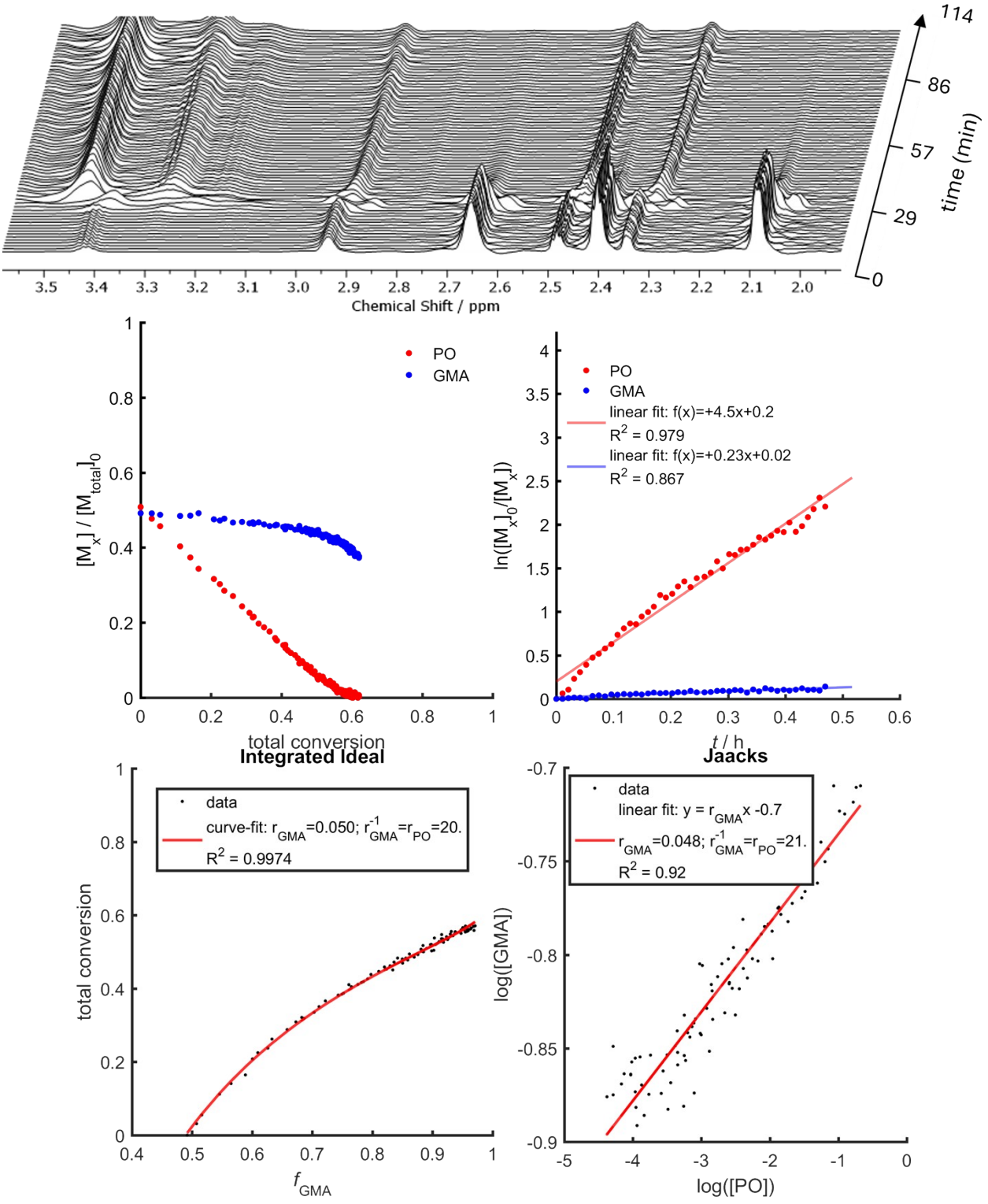

Figure S16. ^{1}H NMR PO-GMA copolymerization experiment: Data with fits to obtain reactivity ratios. Only monomer conversion data in the time interval after the induction period until complete conversion of PO were fitted.

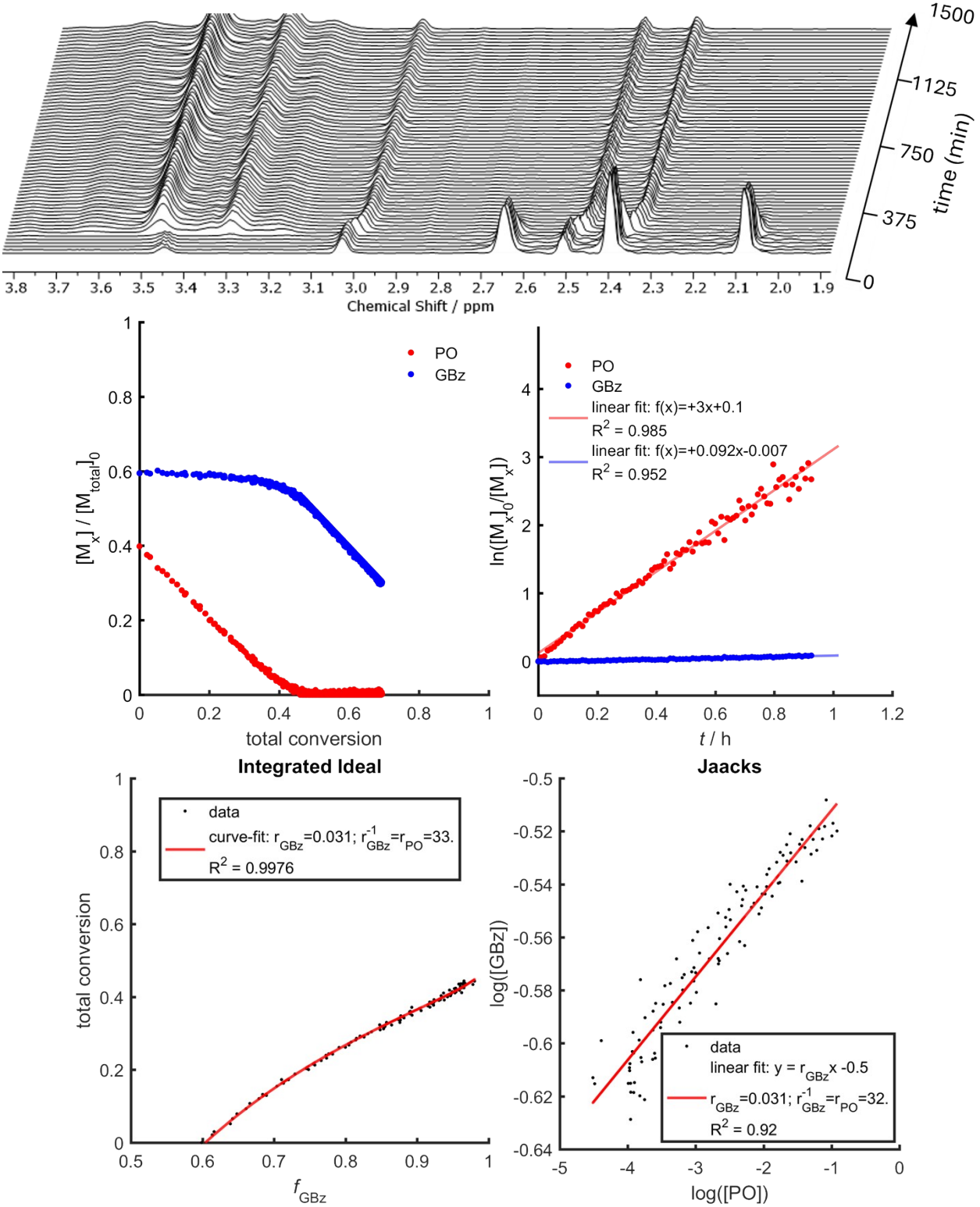

Figure S17. ^{1}H NMR PO-GBz copolymerization experiment: Data with fits to obtain reactivity ratios. Only monomer conversion data in the time interval after the induction period until complete conversion of PO were fitted.

SEC traces of glycidyl ether and glycidyl ester copolymers

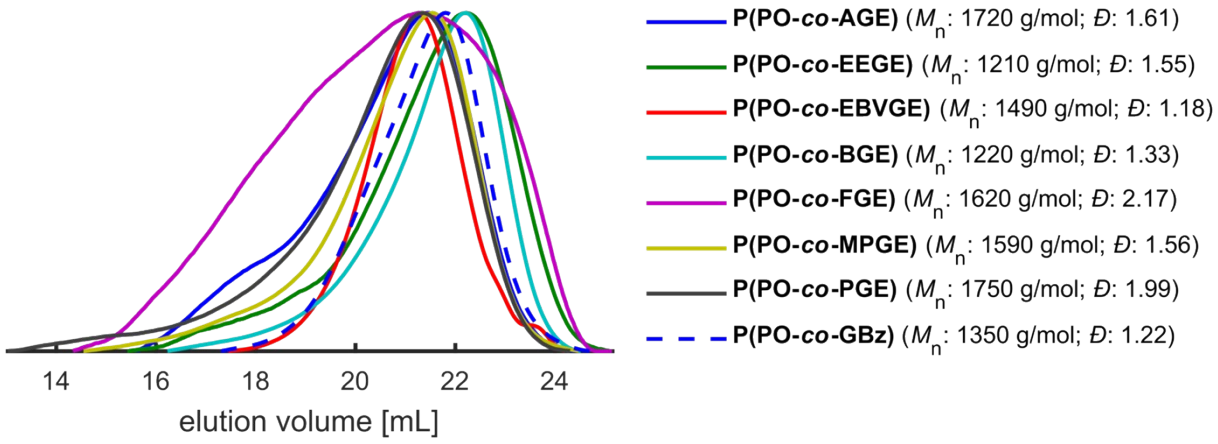

Figure S18. SEC traces (DMF, PEG-calibration) of copolymerization experiments of PO with glycidyl ethers (lines) and the glycidyl ester GBz (dashed line).

DFT Calculations

DFT calculations were performed with the software *ORCA 6.1.0* at the B3LYP-D4 level.[5] The def2-TZVP valence triple-zeta basis set with polarization functions was used to represent the molecular orbitals/electron density for all atoms.[6] The DefGrid2 numerical integration grid (default) and TightSCF convergence were used throughout geometry optimizations and harmonic frequency calculations. Optimizations were unconstrained and employed the standard geometry optimizer of the software with default convergence thresholds. For each optimized structure, analytic harmonic frequency calculations (Freq) were performed at the same level to verify true minima (no imaginary frequencies). Where noted, solvation was modeled with the conductor-like polarizable continuum CPCM (benzene, ε = 2.2706).[7] Hirshfeld atomic charges were reported as Boltzmann-weighted averages over the optimized potential conformers in each medium.[8]

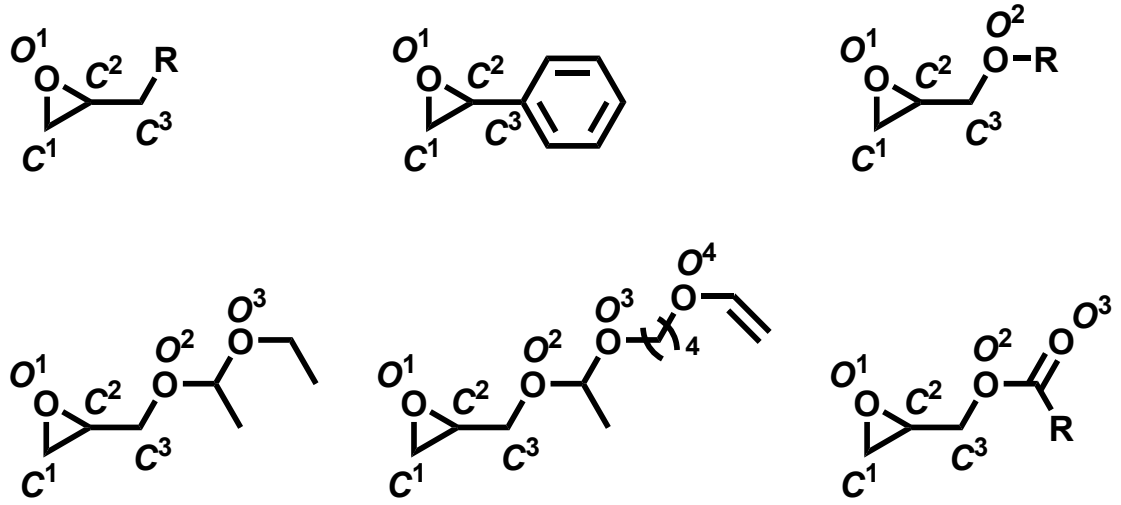

Scheme S3. Assigned labels for atomic charges O^1, C^1, C^2 and C^3 in alkylene oxides and aryl epoxides and additionally O^2, O^3, O^4 in glycidyl ethers, glycidyl ether acetals and glycidyl esters.

Table S4. Hirshfeld atomic charges of epoxide-ring atoms computed for optimized geometries of alkylene oxides and aryl epoxide monomers (AO).

Monomer Structure	$(O^1)^v$ /e	$(C^1)^v$ /e	$(C^2)^v$ /e	$(C^3)^v$ /e	$(O^1)^b$ /e	$(C^1)^b$ /e	$(C^2)^b$ /e	$(C^3)^b$ /e
	-0.202	0.021	0.021	-	-0.222	0.022	0.022	-
	-0.208	0.016	0.051	-0.068	-0.228	0.017	0.052	-0.069
	-0.206	0.016	0.048	-0.034	-0.225	0.017	0.049	-0.034
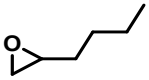	-0.205	0.016	0.048	-0.037	-0.224	0.017	0.050	-0.037
	-0.204	0.016	0.047	-0.002	-0.223	0.017	0.048	-0.002
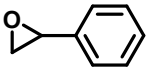	-0.191	0.023	0.048	0.000	-0.207	0.025	0.048	-0.003
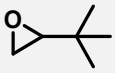	-0.201	0.016	0.047	0.028	-0.219	0.017	0.048	0.029

[v]vacuum.
[b]solvent: benzene.

Table S5. Hirshfeld atomic charges of epoxide-ring atoms computed for optimized geometries of glycidyl ether (GE) and glycidyl ester (GEs) monomers.

Monomer Structure	$(O^1)^v$ /e	$(C^1)^v$ /e	$(C^2)^v$ /e	$(C^3)^v$ /e	$(O^1)^b$ /e	$(C^1)^b$ /e	$(C^2)^b$ /e	$(C^3)^b$ /e
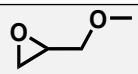	-0.200	0.020	0.045	0.041	-0.218	0.022	0.046	0.040
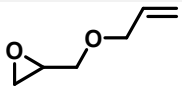	-0.201	0.020	0.045	0.039	-0.218	0.021	0.046	0.039
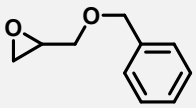	-0.202	0.019	0.044	0.040	-0.219	0.020	0.045	0.039
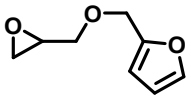	-0.201	0.019	0.045	0.038	-0.218	0.021	0.045	0.037
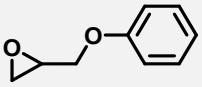	-0.198	0.023	0.048	0.048	-0.216	0.024	0.048	0.048
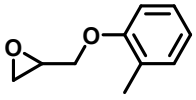	-0.198	0.022	0.048	0.048	-0.217	0.024	0.048	0.049
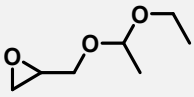	-0.203	0.020	0.044	0.040	-0.220	0.021	0.044	0.039
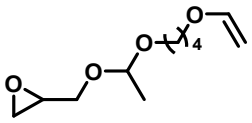	-0.204	0.019	0.044	0.040	-0.221	0.020	0.044	0.039
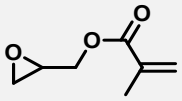	-0.199	0.023	0.044	0.049	-0.216	0.024	0.046	0.049
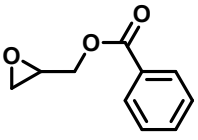	-0.199	0.023	0.044	0.049	-0.216	0.025	0.046	0.050

[v]vacuum.
[b]solvent: benzene.

Table S6. Hirshfeld atomic charges of oxygen atoms in glycidyl ether (GE) and glycidyl ester (GEs) monomers.

Monomer Structure	$(O^1)^v$ /e	$(O^2)^v$ /e	$(O^3)^v$ /e	$(O^4)^v$ /e	$(O^1)^b$ /e	$(O^2)^b$ /e	$(O^3)^b$ /e	$(O^4)^b$ /e
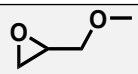	-0.200	-0.187	-	-	-0.218	-0.198	-	-
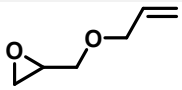	-0.201	-0.185	-	-	-0.218	-0.196	-	-
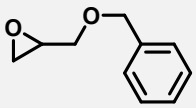	-0.202	-0.180	-	-	-0.219	-0.189	-	-
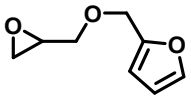	-0.201	-0.182	-0.101	-	-0.218	-0.194	-0.105	-
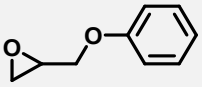	-0.198	-0.145	-	-	-0.216	-0.151	-	-
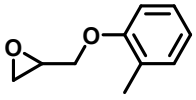	-0.198	-0.134	-	-	-0.217	-0.141	-	-
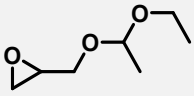	-0.203	-0.179	-0.186	-	-0.220	-0.186	-0.191	-
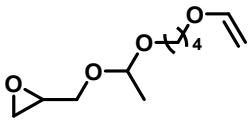	-0.204	-0.178	-0.181	-0.139	-0.221	-0.185	-0.189	-0.146
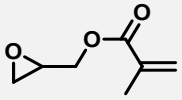	-0.199	-0.127	-0.280	-	-0.216	-0.129	-0.298	-
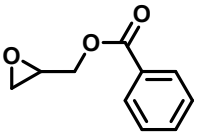	-0.199	-0.126	-0.282	-	-0.216	-0.127	-0.300	-

[v]vacuum.
[b]solvent: benzene.

Frontier orbital energies (HOMO and LUMO) were taken from the Kohn–Sham eigenvalues of single-point SCF calculations at the same DFT-level (B3LYP-D4/ def2-TZVP) and were evaluated on the optimized geometries in benzene. The orbital energies and HOMO-LUMO gaps are reported in eV. Following the Parr–Pearson (HSAB) conceptual-DFT framework, Mulliken electronegativity (χ) and absolute hardness (η) were evaluated via the Koopmans finite-difference relations ((Eq. S1 and (Eq. S2) The fractional electron transfer (ΔN) was estimated by the Pearson charge-transfer expression ((Eq. S3).[9,10]

$$\chi \approx -\frac{\varepsilon_{HOMO} + \varepsilon_{LUMO}}{2} \quad \text{(Eq. S1)}$$

$$\eta \approx \frac{\varepsilon_{LUMO} - \varepsilon_{HOMO}}{2} \quad \text{(Eq. S2)}$$

$$\Delta N = \frac{\chi_{Zn} - \chi_{Lig}}{2(\eta_{Zn} + \eta_{Lig})} \quad \text{(Eq. S3)}$$

Table S7. Computed parameters for calculation of fractional electron transfer of alkylene oxide or aryl epoxide monomer towards Zn^{2+}.

Monomer	$\boldsymbol{\varepsilon_{HOMO}}$ **/eV**	$\boldsymbol{\varepsilon_{LUMO}}$ **/eV**	$\boldsymbol{\varepsilon_{Gap}}$ **/eV**	χ **/eV**	η **/eV**	ΔN
EO	-7.575	1.637	9.212	2.969	4.606	0.078
PO	-7.462	1.451	8.913	3.006	4.457	0.077
BO	-7.432	1.327	8.759	3.053	4.380	0.075
HexO	-7.422	1.136	8.558	3.143	4.279	0.071
MEB	-7.407	1.140	8.547	3.134	4.274	0.071
SO	-6.724	-0.548	6.176	3.636	3.088	0.051
DMEB	-7.377	1.017	8.394	3.180	4.197	0.069
Zn^{2+*}	-9.390	0.490	9.880	4.450	4.940	-

*values previously reported by Pearson.[9]

Table S8. Computed parameters for calculation of the fractional electron transfer of glycidyl ether or glycidyl ester monomer towards Zn^{2+}.

Monomer	ε_{HOMO} **/eV**	ε_{LUMO} **/eV**	ε_{Gap} **/eV**	χ **/eV**	η **/eV**	ΔN
GME	-7.093	1.514	8.607	2.790	4.304	0.090
AGE	-7.078	-0.050	7.028	3.564	3.514	0.052
BGE	-6.845	-0.540	6.305	3.693	3.153	0.047
FGE	-6.403	-0.231	6.172	3.317	3.086	0.071
PGE	-6.246	-0.401	5.845	3.324	2.923	0.072
MPGE	-6.065	-0.208	5.857	3.137	2.929	0.083
EEGE	-7.218	1.018	8.236	3.100	4.118	0.075
EBVGE	-6.346	0.320	6.666	3.013	3.333	0.087
GMA	-7.479	-1.417	6.062	4.448	3.031	0.000
GBz	-7.251	-1.550	5.701	4.401	2.851	0.003
Zn^{2+*}	-9.390	0.490	9.880	4.450	4.940	-

*values previously reported by Pearson.[9]

Buried volume $\%V_{Bur}$ and steric maps of monomers

The percentage buried volume ($\%V_{Bur}$) was computed for each comonomer with the web tool *SambVca 2.1* using the previously optimized monomer geometries.[11] For the epoxide oxygen (O^1), $\%V_{Bur}(O^1)$ was evaluated by placing a 3.5 Å radius sphere centered on O^1; the corresponding topographic steric maps were generated along the $+Z$ viewing direction, defined as the expected approach vector for coordination of O^1 to the catalyst's active Zn site. Analogously, $\%V_{Bur}(C^1)$ for the unsubstituted methylene carbon of the epoxide ring and its steric map were calculated using the same sphere and +Z orientation, corresponding to the trajectory of nucleophilic attack that drives ring opening by the initiator or the propagating polymer chain.

Table S9. Computed total $\%V_{Bur}$ around oxygen (O_1) and unsubstituted methylene carbon (C_1) for optimized geometry of alkylene oxides and aryl epoxides (AO).

Monomer	Structure	$\%V_{Bur}(O_1)$	t_i /min	$\%V_{Bur}(C_1)$	r_{AO}
EO[12]		34.5	< 1.5	34.5	0.42
PO-d_6*	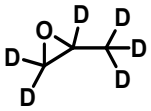	43.4	-	39.0	1.0
BO		45.4	18	39.4	0.21
HexO	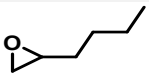	47.4	37	41.7	0.063
SO	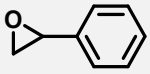	48.4	26	41.8	0.047
MEB		49.3	39	41.9	0.034
DMEB	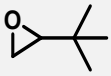	53.1	40	44.5	≈ 0

Table S10. Computed total $\%V_{Bur}$ around oxygen (O_1) and unsubstituted methylene carbon (C_1) for optimized geometry of glycidyl ethers (GE) and glycidyl esters (GEs).

Monomer	Structure	$\%V_{Bur}(O_1)$	t_i /min	$\%V_{Bur}(C_1)$	r_{AO}
GME	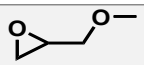	46.8	-	40.3	1.4
AGE	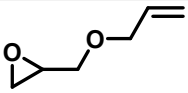	46.8	8	40.3	9.2
BGE	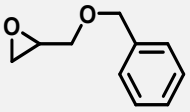	44.6	75	39.2	12
FGE	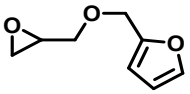	44.7	104	39.5	14
PGE	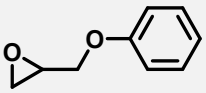	45.6	235	40.4	14
MPGE	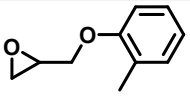	44.7	116	39.5	17
EEGE	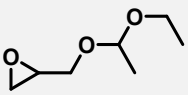	53.4	76	45.8	21
EBVGE*	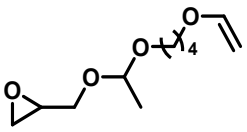	-	29	-	16
GMA	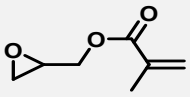	46.2	40	39.6	0.050
GBz	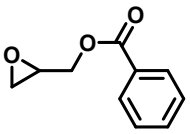	46.2	77	39.6	0.031

*$\%V_{Bur}$ values not reported, extensive conformational flexibility of molecule renders values inaccurate.

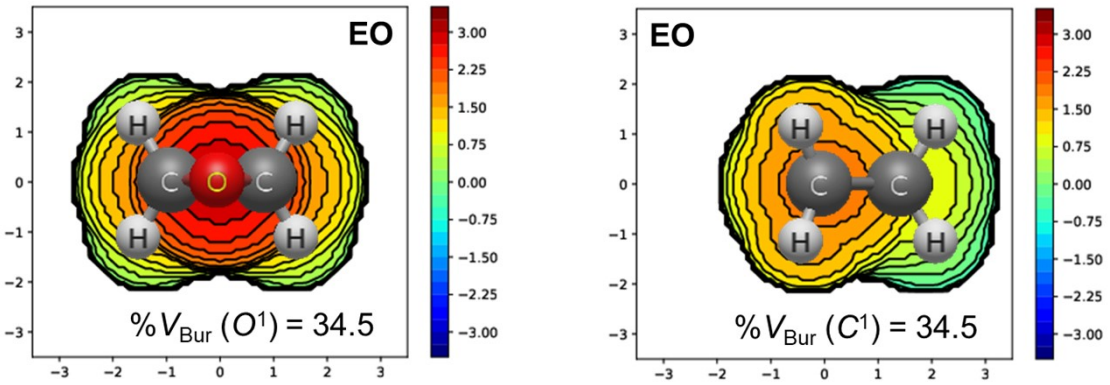

Figure S19. Topographic steric maps of EO. Left: In +*Z* viewing direction with oxygen O^1 placed in center. Right: In +*Z* viewing direction with oxygen C^1 placed in center.

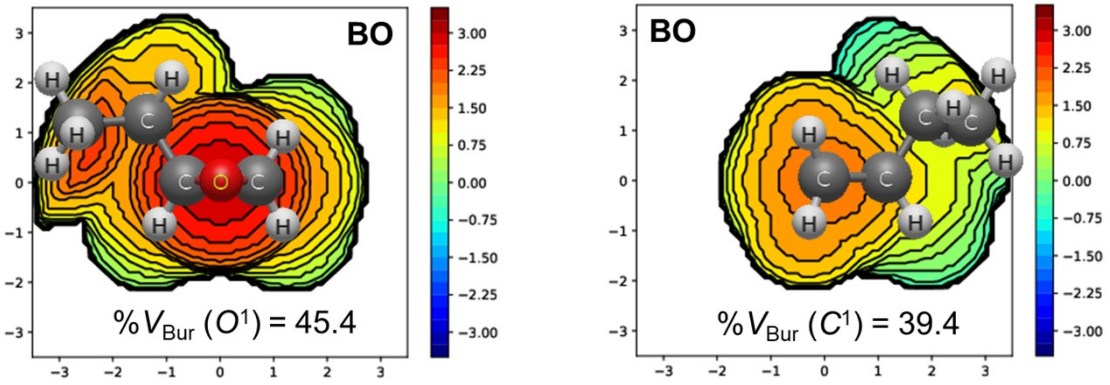

Figure S20. Topographic steric maps of BO. Left: In +*Z* viewing direction with oxygen O^1 placed in center. Right: In +*Z* viewing direction with oxygen C^1 placed in center.

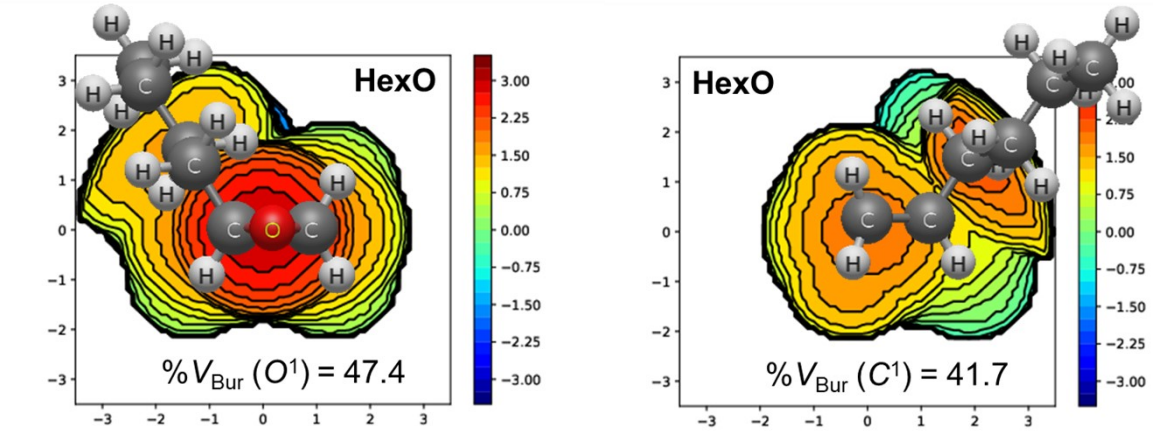

Figure S21. Topographic steric maps of HexO. Left: In +*Z* viewing direction with oxygen O^1 placed in center. Right: In +*Z* viewing direction with oxygen C^1 placed in center.

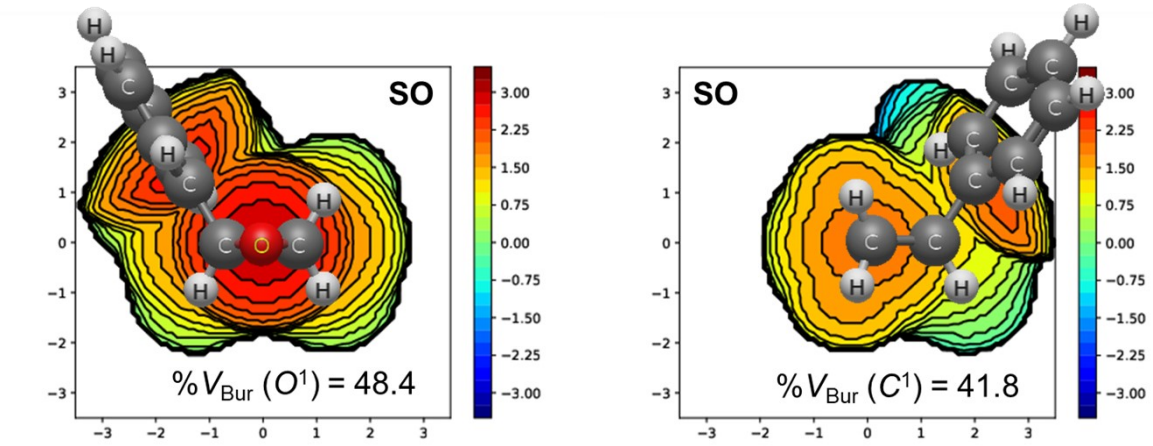

Figure S22. Topographic steric maps of SO. Left: In +*Z* viewing direction with oxygen O^1 placed in center. Right: In +*Z* viewing direction with oxygen C^1 placed in center.

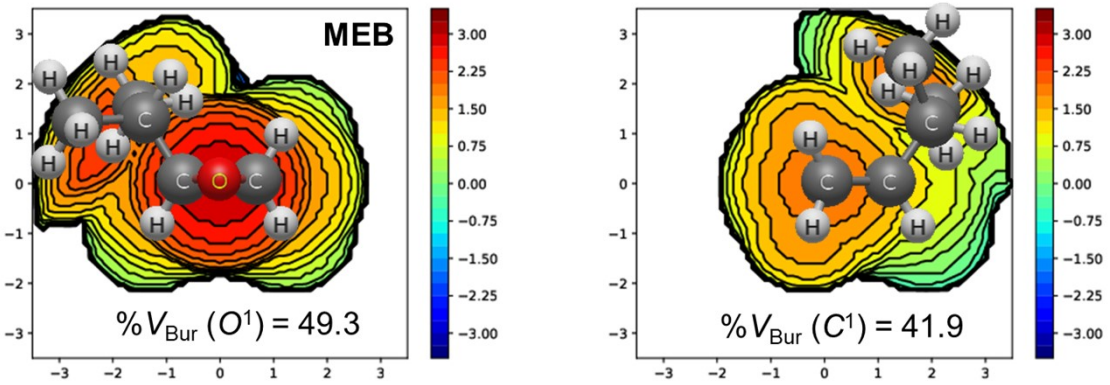

Figure S23. Topographic steric maps of MEB. Left: In +*Z* viewing direction with oxygen O^1 placed in center. Right: In +*Z* viewing direction with oxygen C^1 placed in center.

Cartesian coordinates of optimized monomer geometries in benzene

(EO) Atoms	**7**		
E	-153.772862		
Element	X	Y	Z
C	-12.91209213	3.005563212	-9.019025126
C	-13.16554449	3.765665784	-7.795451643
O	-14.11059814	2.794317993	-8.261987727
H	-12.20576785	2.181469789	-9.001096377
H	-13.05608182	3.480709441	-9.984336712
H	-13.494876	4.797707061	-7.86454892
H	-12.64477958	3.49829672	-6.881313495

(PO) Atoms	**10**		
E	-193.0838485		
Element	X	Y	Z
C	-12.90062873	3.208492835	-8.920756621
C	-13.28887041	4.036840666	-7.778897057
O	-13.52689961	2.618430539	-7.770463508
H	-11.85432625	2.949527815	-9.055910248
H	-13.50336822	3.208784505	-9.823940632
C	-12.29070029	4.557607972	-6.786625169
H	-14.20180801	4.620693873	-7.877383358
H	-11.4052009	3.920788568	-6.757776302
H	-12.72624103	4.592577545	-5.785381609
H	-11.98385656	5.571425684	-7.055855496

(BO) Atoms	**13**		
E	-232.3871301		
Element	X	Y	Z
C	-7.497151154	2.924931643	0.896431916
C	-7.774007018	1.765580372	0.049324295
C	-9.035855688	1.632229887	-0.757120863
O	-7.913468742	1.680315504	1.479951732
H	-6.918842256	1.206296702	-0.327639947
H	-8.228916092	3.725561848	0.954644735
H	-6.471451237	3.212284919	1.107229678
C	-9.523282006	0.185484598	-0.838809577
H	-8.842172881	2.019673079	-1.763068838
H	-9.80768594	2.266803081	-0.313071917
H	-8.771025244	-0.457264979	-1.302915961
H	-10.43723056	0.112723731	-1.431001929
H	-9.733931181	-0.208640386	0.157316677

(MEB) Atoms	**16**		
E	-271.6922723		
Element	X	Y	Z
C	-7.542106702	2.790355397	-2.294741917
C	-8.571757337	1.769178692	-2.109529479
C	-8.925208891	1.210854418	-0.753667801
O	-7.283966979	1.419923103	-2.642777772
H	-9.370810812	1.721411565	-2.849345395
H	-6.994894725	3.152873754	-1.429169499
H	-7.59764026	3.476117406	-3.134647019
C	-9.247027103	-0.281613063	-0.856452858
H	-10.1204435	-0.446406251	-1.493973586
H	-9.467214776	-0.700071339	0.127923452
H	-8.407548499	-0.83448273	-1.281661871
C	-10.08813278	2.001568912	-0.149608044
H	-8.045152169	1.334187238	-0.113305025
H	-10.98207533	1.918987837	-0.774203588
H	-9.841517163	3.061130979	-0.052303701
H	-10.33960296	1.619604082	0.841764105

(HexO) Atoms	**19**		
E			
Element	X	Y	Z
C	0.7528	0	-0.00184
C	-0.7528	0	0.00184
O	0	0	1.22037
H	1.27643	0.90906	-0.26925
H	1.2645	-0.91499	-0.27258
C	-1.53085	1.25298	-0.24493
H	-1.28129	-0.90394	-0.2692
C	-1.63592	1.54769	-1.74122
H	-1.06384	2.10455	0.26521
H	-2.53316	1.13495	0.18448
C	-2.48172	2.79138	-2.00922
H	-2.07276	0.68501	-2.25912
H	-0.63013	1.68724	-2.15698
C	-2.52549	3.12404	-3.49225
H	-2.07282	3.64824	-1.46147
H	-3.50324	2.63035	-1.64524
H	-1.52192	3.33736	-3.87501
H	-3.14886	4.00671	-3.66502
H	-2.94352	2.29334	-4.06947

(DMEB) Atoms	**19**		
E	-310.9965569		
Element	X	Y	Z
C	-7.308577558	2.649887597	-2.170963246
C	-8.367023742	1.678483245	-1.895407266
C	-8.650716461	1.047636935	-0.54089078
O	-7.178829455	1.282828185	-2.596808194
H	-9.243464731	1.717505076	-2.541908298
H	-6.624849714	2.948667399	-1.38429873
H	-7.438032373	3.370026921	-2.973330197
C	-9.105236109	-0.399633806	-0.786881912
H	-9.982833493	-0.431145711	-1.437533059
H	-9.367124941	-0.884106365	0.156449092
H	-8.310936627	-0.980893975	-1.259449663
C	-9.787114824	1.846841466	0.112214513
H	-10.6816042	1.849432902	-0.515680915
H	-9.489865812	2.884041136	0.284513726
H	-10.05510299	1.407463492	1.075554972
C	-7.41924356	1.049242477	0.37074845
H	-6.567019377	0.574228763	-0.117659912
H	-7.636719272	0.495254447	1.286050812
H	-7.131874763	2.062269815	0.658320606

(SO) Atoms	**17**		
E	-384.7902216		
Element	X	Y	Z
C	-7.760440829	1.890328929	-1.717809877
C	-9.17410607	1.924080869	-2.119155648
C	-10.22462024	1.161907199	-1.396561909
O	-8.208421732	1.175045057	-2.872980779
H	-9.524347406	2.820656751	-2.624151049
H	-7.472179693	1.269040181	-0.875165514
H	-7.122368968	2.745286216	-1.920440211
C	-10.04994374	-0.181987158	-1.064869543
C	-11.40595872	1.804697002	-1.028888782
C	-11.03745457	-0.865325733	-0.367509302
C	-12.39215393	1.12210395	-0.325985772
C	-12.20975816	-0.215226721	0.007763797
H	-10.89435131	-1.909732727	-0.119340345
H	-12.97883783	-0.750485301	0.550316945
H	-9.145416114	-0.691782345	-1.370669568
H	-11.55433814	2.84449743	-1.296871917
H	-13.30488255	1.632856401	-0.045470524

(GME) Atoms	**14**		
E	-307.5919755		
Element	X	Y	Z
C	-7.968754602	1.795579517	-1.666221659
C	-9.250015221	1.468904104	-2.291892834
O	-8.322154223	0.431209874	-1.925060351
H	-7.943458468	2.071703305	-0.615905756
H	-7.1602726	2.188816881	-2.274122909
C	-10.53585612	1.547713458	-1.515902662
H	-9.349178394	1.606597284	-3.366295583
O	-11.57063355	0.744476914	-2.054092381
H	-10.90778201	2.574810115	-1.550727008
H	-10.34271681	1.281712044	-0.467682077
C	-11.36313956	-0.651708066	-1.887604613
H	-12.26679833	-1.148502844	-2.238086696
H	-11.19964097	-0.900538027	-0.832243304
H	-10.50733915	-1.009834557	-2.467142167

(AGE) Atoms	**18**		
E	-384.9720437		
Element	X	Y	Z
C	-8.122967361	1.784931017	-0.95089908
C	-8.937170162	1.598614211	-2.151596972
O	-7.706429709	0.873080053	-1.975503734
H	-8.431589359	1.317997532	-0.019932797
H	-7.514048998	2.677480895	-0.849383975
C	-10.21251503	0.803477531	-2.109609746
H	-8.890018714	2.356125392	-2.930581857
O	-10.58704026	0.275133803	-3.369873199
H	-11.03143077	1.461237638	-1.808089934
H	-10.11573766	0.001246635	-1.3658808
C	-9.752373358	-0.792228059	-3.825339785
C	-10.39567645	-1.41669326	-5.019126132
H	-9.649966666	-1.532516482	-3.018505789
H	-8.749621564	-0.428993796	-4.071506282
C	-9.787409238	-1.593119169	-6.185014991
H	-11.42186712	-1.745868686	-4.880795413
H	-8.766647389	-1.263102131	-6.346044523
H	-10.28344019	-2.078053124	-7.016714989

(BGE) Atoms	**24**		
E	-538.6045961		
Element	X	Y	Z
C	-11.58848605	0.303015061	-6.592874233
C	-10.59362303	0.167528855	-5.534640819
O	-10.42780454	1.151368918	-6.567400854
H	-12.52607231	0.805773129	-6.377100006
H	-11.61622505	-0.42060878	-7.400885382
C	-10.80218473	0.739806859	-4.152487824
H	-9.894021618	-0.662777197	-5.589731534
O	-11.11238377	-0.237318705	-3.170497551
H	-11.57867403	1.514175468	-4.190125556
H	-9.871827664	1.205965107	-3.820506708
C	-12.4533444	-0.716337972	-3.191626273
C	-12.72324157	-1.759457159	-4.250140976
H	-13.14951809	0.122016272	-3.31102381
H	-12.61454503	-1.14546647	-2.199716059
C	-11.84164871	-2.824926544	-4.431767971
C	-13.86078911	-1.68291675	-5.048763484
C	-14.11545098	-2.648519576	-6.017718361
C	-12.08815165	-3.786769871	-5.402247587
H	-10.95203947	-2.889443354	-3.817580497
C	-13.22675066	-3.701304231	-6.199401291
H	-11.3935073	-4.606678273	-5.537503118
H	-13.418538	-4.451070134	-6.956750665
H	-14.54894192	-0.855200872	-4.919351851
H	-15.00253028	-2.572863783	-6.634417589

(FGE) Atoms	**21**		
E	-536.3994473		
Element	X	Y	Z
C	-8.029961736	2.48441565	-4.691423282
C	-8.601501474	1.223594111	-4.221537224
O	-8.405927046	2.321053546	-3.317243308
H	-8.649651195	3.174057389	-5.257234811
H	-6.962574064	2.55266929	-4.875740647
C	-10.01536963	0.850877868	-4.536580206
H	-7.931881246	0.385382631	-4.045389369
O	-10.4930164	0.005309764	-3.500516726
H	-10.04631117	0.333937263	-5.504352797
H	-10.63365541	1.754591724	-4.610530005
C	-11.87925731	-0.319338229	-3.606432501
C	-12.21796262	-1.175745505	-4.773448903
H	-12.47492418	0.600676271	-3.6433039
H	-12.11864117	-0.852596233	-2.687372294
C	-12.20275016	-2.519196417	-4.977042505
O	-12.59674255	-0.544351877	-5.930235474
C	-12.59192661	-2.736836423	-6.335489155
H	-11.94434562	-3.265359196	-4.243685131
C	-12.81859738	-1.508712985	-6.863626546
H	-12.69530092	-3.680659667	-6.84462737
H	-13.13235209	-1.165808975	-7.834277844

(PGE) Atoms	**21**		
E	-499.3055412		
Element	X	Y	Z
C	-10.02594839	3.042576914	-3.267891098
C	-10.4616005	1.903270846	-2.463131888
O	-9.304116991	2.654291148	-2.086207277
H	-10.56132744	3.983749797	-3.189108874
H	-9.501795086	2.870879015	-4.20214989
C	-11.62443176	2.016747392	-1.518755326
H	-10.25262052	0.900078945	-2.825835432
O	-12.77523169	1.565981967	-2.224437851
H	-11.74343048	3.056308511	-1.19747164
H	-11.45472128	1.394274403	-0.633544533
C	-13.96940454	1.528260768	-1.566680759
C	-15.0528946	1.03812909	-2.29948847
C	-14.15086595	1.945522158	-0.249298246
C	-16.30708276	0.966935576	-1.715732356
C	-16.49966154	1.380736283	-0.39827855
C	-15.4189662	1.866681111	0.323698801
H	-17.1406776	0.585348672	-2.292225786
H	-17.48042086	1.323569166	0.055436486
H	-14.88944025	0.719734454	-3.321057573
H	-13.3261141	2.329634853	0.332747609
H	-15.55313747	2.192398931	1.347852654

(MPGE) Atoms	**24**		
E	-538.6144304		
Element	X	Y	Z
C	-9.009515533	1.42232736	-1.641210459
C	-10.31739781	1.549995665	-2.282016916
O	-9.732896365	0.259125904	-2.064700624
H	-8.925962541	1.543831541	-0.565195482
H	-8.112938226	1.644646258	-2.210597816
C	-11.53575466	1.878547898	-1.479338814
H	-10.35801347	1.846295586	-3.327076719
O	-12.65505148	1.307805949	-2.14685249
H	-11.65159275	2.966744226	-1.410920091
H	-11.44102244	1.469081624	-0.468809891
C	-13.89728995	1.474488873	-1.606556645
C	-14.94928504	0.880107211	-2.324054743
C	-14.14221934	2.177197106	-0.429968379
C	-16.23785878	1.017235475	-1.823899238
C	-16.49858859	1.718749393	-0.648213902
C	-15.44688015	2.296415068	0.044649066
H	-17.05634937	0.562198556	-2.369796863
H	-17.51329046	1.808767431	-0.282496324
H	-13.33272646	2.631552433	0.122172128
H	-15.62909649	2.84441898	0.96068597
C	-14.66583503	0.123885911	-3.589996712
H	-15.58756925	-0.276451634	-4.011776745
H	-13.97732092	-0.705490504	-3.410959998
H	-14.19342489	0.765343692	-4.338158315

(EEGE) Atoms	**24**		
E	-500.7309557		
Element	X	Y	Z
C	-10.09840859	-0.676172958	-1.820977116
C	-11.55334652	-0.543359701	-1.854045923
O	-10.91692996	-1.376672898	-0.87150275
H	-9.501757043	0.130114463	-1.404691768
H	-9.599315361	-1.306310762	-2.550124434
C	-12.21781792	0.695818377	-1.304901249
H	-12.1032762	-1.092770062	-2.609953944
O	-12.20773769	1.78995949	-2.217055559
H	-11.66311972	1.021644515	-0.423478299
H	-13.24745847	0.470784548	-1.003046141
C	-13.25739641	1.810237961	-3.161460235
O	-13.1335528	0.779628031	-4.122285615
C	-13.30226317	3.206994057	-3.751288038
H	-14.20062218	1.573159124	-2.65684027
H	-12.32926392	3.498479959	-4.146925945
H	-13.58241056	3.919353665	-2.975350857
H	-14.04124098	3.249947758	-4.552068638
C	-12.02298942	0.872371526	-5.020271295
C	-11.91926956	-0.437680511	-5.771774064
H	-11.10572333	1.071583178	-4.458655756
H	-12.17756793	1.699707324	-5.720599864
H	-11.72495605	-1.266090483	-5.088480466
H	-11.10316838	-0.390255481	-6.495782643
H	-12.84501782	-0.646951121	-6.310999132

(EBVGE) Atoms	**35**		
E	-731.9321922		
Element	X	Y	Z
C	-15.16313936	3.243862538	-8.025399198
C	-14.39736214	2.268332917	-7.253597287
O	-14.36046326	2.253540468	-8.690145782
H	-14.7938584	4.261845647	-8.108000532
H	-16.23407111	3.12270359	-8.135919467
C	-13.1011932	2.666137963	-6.589141638
H	-14.92888115	1.42964595	-6.818028036
O	-13.2773545	3.380611625	-5.368302307
H	-12.56368174	3.337792774	-7.260037146
H	-12.47870164	1.780670153	-6.413231339
C	-13.5637831	2.594319457	-4.232655517
O	-14.87017856	2.051392293	-4.273609821
C	-15.94667578	2.9888692	-4.210244878
C	-17.21990722	2.267783864	-4.6135489
H	-15.7424562	3.828874106	-4.878884171
H	-16.04336284	3.381313514	-3.190699241
C	-18.4796042	3.121115296	-4.447086493
H	-17.31798532	1.370301968	-3.997366841
H	-17.13217974	1.934074214	-5.649057686
C	-18.5198373	4.380337893	-5.291786296
H	-18.58737456	3.42718963	-3.401371502
H	-19.35674486	2.514777574	-4.687034932
O	-18.45571773	4.012123045	-6.676563648
H	-17.68368101	5.048385744	-5.06038309
H	-19.45062453	4.926870158	-5.108666285
C	-18.41329617	5.044448529	-7.555800644
C	-18.56057984	4.876343113	-8.865420671
H	-18.22711197	6.021523425	-7.116814856
H	-18.74908299	3.901680276	-9.296583951
H	-18.48595622	5.72834234	-9.524883801
C	-13.2905556	3.451546654	-3.011449625
H	-12.92078704	1.70699654	-4.233762267
H	-13.837574	4.393306102	-3.061797905
H	-12.22579103	3.678472205	-2.958032635
H	-13.58276567	2.916709235	-2.107151615

(GMA) Atoms	**20**		
E	-498.337826		
Element	X	Y	Z
C	-12.66229608	5.399305855	-8.279651389
C	-13.2064409	4.244005547	-7.566098238
O	-12.6711362	4.103007289	-8.890488518
H	-11.67844634	5.776513873	-8.016100927
H	-13.34225929	6.123843915	-8.715629258
C	-12.42604681	3.595173102	-6.464071173
H	-14.28480674	4.131080076	-7.509797679
O	-12.66278975	2.172901027	-6.419946628
H	-12.68702299	4.037236136	-5.502347523
H	-11.35767082	3.696841138	-6.645523989
C	-13.75967756	1.756591685	-5.759376098
O	-14.52734028	2.514276051	-5.20667713
C	-13.93902017	0.277223703	-5.770444767
C	-13.10412094	-0.513454457	-6.445070478
H	-12.26850207	-0.11526949	-7.002456313
H	-13.24637585	-1.587195318	-6.455022621
C	-15.11605259	-0.227779557	-4.989307605
H	-16.04654886	0.200902238	-5.367313201
H	-15.04113652	0.063756575	-3.939414747
H	-15.17762924	-1.313639388	-5.049811717

(GBz) Atoms	**23**		
E	-612.6628156		
Element	X	Y	Z
C	-12.9249315	4.89200802	-8.411274155
C	-13.40847474	3.833989863	-7.524220686
O	-12.92182664	3.524111552	-8.838484088
H	-11.94220878	5.323002738	-8.243659603
H	-13.64118987	5.534600545	-8.912675408
C	-12.56711298	3.360320863	-6.378851943
H	-14.48005816	3.705419185	-7.406477365
O	-12.75602586	1.950152871	-6.138199911
H	-12.80672917	3.918710525	-5.473765505
H	-11.50990575	3.465313889	-6.615111239
C	-13.81547984	1.593599992	-5.387445271
O	-14.59080054	2.394120524	-4.912975345
C	-13.91605364	0.122344861	-5.210491168
C	-13.01710359	-0.760816183	-5.812190287
C	-14.95091627	-0.37532096	-4.416563687
C	-13.15530999	-2.12833941	-5.6179661
H	-12.21829532	-0.376153505	-6.429471067
C	-15.08451765	-1.742120565	-4.223582592
C	-14.18680767	-2.620266216	-4.82425874
H	-15.64038333	0.320107355	-3.957835667
H	-15.88749116	-2.124168714	-3.606324542
H	-14.29175892	-3.687569908	-4.674314016
H	-12.45815863	-2.811307323	-6.086291613

References

1 A. O. Fitton, J. Hill, D. E. Jane and R. Millar, *Synthesis*, 1987, **1987**, 1140–1142.

2 a) K. Maciol, T. Dänzer, J. Keth, J. Blankenburg and H. Frey, *to be submitted*; b) K. Maciol, Dissertation, Johannes Gutenberg-Universität, 2018;

3 J. Leuschner, H. Schäfer and F. Leuschner, *Eur. J. Med. Chem.*, 1994, **29**, 241–243.

4 D. A. Pyatakov and I. E. Nifant'ev, *Pet. Chem.*, 2023, **63**, 1170–1193.

5 a) F. Neese, *WIREs Comput Mol Sci*, 2012, **2**, 73–78; b) F. Neese, *WIREs Comput Mol Sci*, 2025, **15**; c) A. D. Becke, *J. Chem. Phys.*, 1993, **98**, 1372–1377; d) C. Lee, W. Yang and R. G. Parr, *Phys. Rev. B*, 1988, **37**, 785–789; e) E. Caldeweyher, J.-M. Mewes, S. Ehlert and S. Grimme, *PCCP*, 2020, **22**, 8499–8512; f) E. Caldeweyher, S. Ehlert, A. Hansen, H. Neugebauer, S. Spicher, C. Bannwarth and S. Grimme, *J. Chem. Phys.*, 2019, **150**, 154122; g) L. Wittmann, I. Gordiy, M. Friede, B. Helmich-Paris, S. Grimme, A. Hansen and M. Bursch, *PCCP*, 2024, **26**, 21379–21394;

6 a) F. Weigend and R. Ahlrichs, *PCCP*, 2005, **7**, 3297–3305; b) A. Schäfer, H. Horn and R. Ahlrichs, *J. Chem. Phys.*, 1992, **97**, 2571–2577;

7 M. Garcia-Ratés and F. Neese, *J. Comput. Chem.*, 2020, **41**, 922–939.

8 F. L. Hirshfeld, *Theoret. Chim. Acta*, 1977, **44**, 129–138.

9 R. G. Pearson, *J. Am. Chem. Soc.*, 1985, **107**, 6801–6806.

10 C. H. Tran, H. B. Jang, B. Moon, E. Lee, H. Choi and I. Kim, *Catal. Today*, 2024, **425**, 114319.

11 a) L. Falivene, R. Credendino, A. Poater, A. Petta, L. Serra, R. Oliva, V. Scarano and L. Cavallo, *Organometallics*, 2016, **35**, 2286–2293; b) L. Falivene, Z. Cao, A. Petta, L. Serra, A. Poater, R. Oliva, V. Scarano and L. Cavallo, *Nat. Chem.*, 2019, **11**, 872–879;

12 J. Blankenburg, E. Kersten, K. Maciol, M. Wagner, S. Zarbakhsh and H. Frey, *Polym. Chem.*, 2019, **10**, 2863–2871.